EXPRESSION AND PURIFICATION OF NON-PROLYL CIS-PEPTIDE BOND MUTANTS IN HUMAN PLASMA PLATELET ACTIVATING FACTOR ACETYLHYDROLASE

by

Kaitlyn Woerner

A dissertation submitted to the Faculty of the University of Delaware in partial fulfillment of the requirements for the degree of Master of Science in Chemistry and Biochemistry

Spring 2015

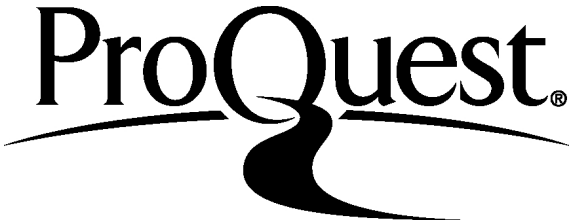

EXPRESSION AND PURIFICATION OF NON-PROLYL CIS-PEPTIDE BOND MUTANTS IN HUMAN PLASMA PLATELET ACTIVATING FACTOR ACETYLHYDROLASE

by

Kaitlyn Woerner

Approved: _____
Brian J. Bahnson, Ph.D.
Professor in charge of thesis on behalf of Advisory Committee

Approved: _____
Murray V. Johnston, Ph.D.
Chair of the Department of Chemistry and Biochemistry

Approved: _____
George H. Watson, Ph.D.
Dean of the College of Arts and Sciences

Approved: _____
James G. Richards, Ph.D.
Vice Provost for Graduate and Professional Education

TABLE OF CONTENTS

LIST OF FIGURES

LIST OF TABLES

LIST OF ABBREVIATIONS

AAG	1-O-alkyl-2-acetyl-sn-glycerol
ATP	Adenosine-5'-triphosphate
BF1	Brain factor-1
BSA	Bovine serum albumin
DFP	Disopropylfluorophosphate
DTT	Dithiothreitol
EDTA	Ethylenediamine-N,N,N',N'-tetraacetic acid
GA	Tabun
GB	Sarin
GD	Soman
GF	Cyclosarin
GST	Glutathione S-transferase
HDL	High density lipoproteins
IPTG	Isopropyl--d-thiogalactopyranoside

LB	Luria-Bertani media
LDL	Low density lipoproteins
Lp(a)	Lipoprotein (a)
Lyso-PAF	Lyso-platelet activating factor, 1-O-alkyl-sn-glycero-3-phosphocholine
OP	Organophosphorous
PAF	Platelet activating factor
PAF-AH	Platelet activating factor acetyl hydrolase
PAF-AH2	Platelet activating factor acetyl hydrolase 2
PAF-AH1B	Platelet activating factor acetyl hydrolase 1 b
PCR	Polymerase chain reaction
pI	Isoelectric point
PNPA	P-nitrophenyl acetate
SDS	Sodium dodecyl sulfate
TFE	Trifluoroethanol

ABSTRACT

Platelet activating factor acetylhydrolase (PAF-AH) is a protein that is found in blood plasma and is associated with lipoproteins. PAF-AH is a calcium-independent serine esterase that functions on the lipid-aqueous interface and is known to degrade platelet-activating factor (PAF) by hydrolyzing the ester bond at the sn-2 position to produce the biologically inactive products lyso-PAF and acetate. In addition to PAF, PAF-AH is also capable of hydrolyzing other substrates, such as oxidized phosphatidylcholine. The cleavage of oxidized phosphatidylcholine produces lysophosphatidylcholine and oxidized nonesterified fatty acids, which are proinflammatory and proapoptotic lipid mediators. The buildup of these proinflammatory lipids is believed to support atherosclerotic plaque expansion, as well as the establishment and advancement of the necrotic centers of atherosclerosis.

PAF-AH has a non-prolyl cis peptide bond between Phe-72 and Asp-73 that is located in a β-hairpin type IV that extends from Ser-64 to Ser-87. The existence a non-prolyl cis peptide bond at this location serves

no known purpose, however trans-cis isomerization may complicate the folding kinetics and create a transient population of partially folded intermediates. This heterogeneity in the unfolded state of the protein may give rise to a series of slow-folding reactions that dramatically slow the overall rate of protein folding and contribute to the high activation barrier of isomerization. In addition, protein heterogeneity may hinder the production of diffraction quality crystals.

In this study, a series of three mutations were produced at the site of the non-prolyl cis peptide bond in an effort to create a more homogenous plasma PAF-AH protein sample and possibly increase the overall yield of pure protein. Furthermore, an additional series of mutations were produced to enhance the somanase activity of plasma PAF-AH. These mutations were made to facilitate the formation of a catalytic triad to aid in the hydrolysis of soman by plasma PAF-AH.

Chapter 1

INTRODUCTION

1.1 Cis-Peptide Bonds in Proteins

Proteins are large biological molecules that consist of long chains of amino acids. All amino acids have the same basic structure, consisting of a sequence of N, Cα, C, and O atoms, which in turn give rise to the backbone of the protein. Amino acids differ only in their side-chains or R-group, which allows each amino acid to have its own properties and biological functions. The protein backbone is comprised of three recurring dihedral angles. The phi torsion angle (ϕ) defines the rotation of the polypeptide chain around the N-Cα bond. The psi torsion angle (ψ) defines the rotation of the polypeptide chain around the Cα-C bond. Lastly, the omega torsion angle (ω) defines the rotation of the polypeptide around the C-N bond (Figure 1.1) [1].

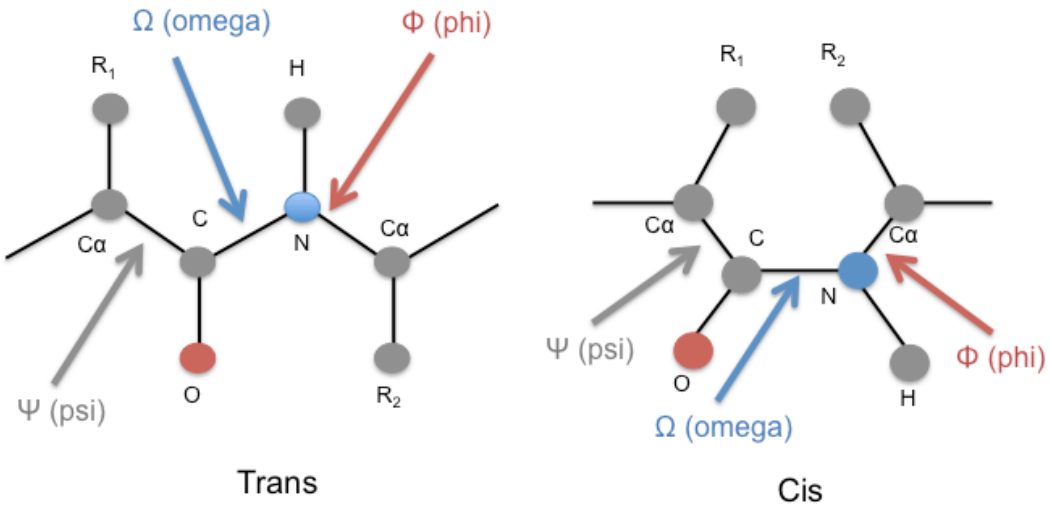

Figure 1.1 Peptide bonds in the trans and cis conformation showing their three dihedral torsion angles.

The delocalization of the carbonyl π electrons and the nitrogen lone pair electrons give the peptide linkage partial double bond character. Therefore, the peptide bond is rendered planar in either the cis or trans conformation [1]. The vast majority of peptide bonds in protein structures are found in the trans conformation with a ω torsion angle of approximately 180°. However, 0.31% of peptide linkages are observed in the cis conformation with a ω torsion angle of approximately 0° (Figure 1.2) [2]. The trans conformation of peptide bonds is preferred due to decreased steric hindrance between the side chains of adjacent α-carbon atoms. However, this steric hindrance is partially relieved through the slight

distortion of ϕ and ψ backbone dihedral angles near the site of the cis peptide bond [3].

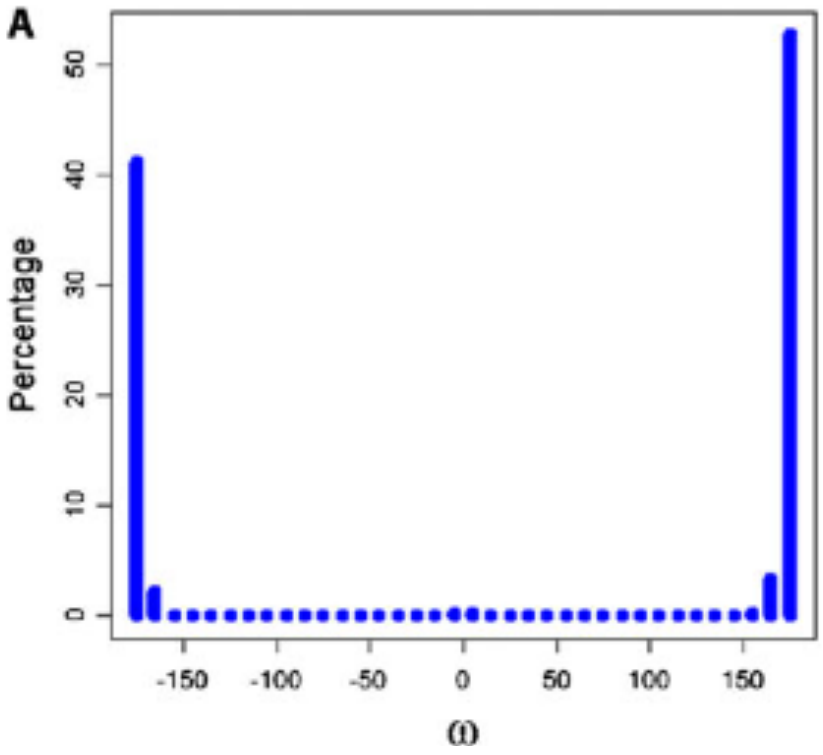

Figure 1.2 The distribution of ω torsion angles of a data set covering 775 protein families. All proteins structures used were solved by X-ray crystallography with resolution better than 1.6 Å and R-factor <0.25. Only 0.31% of all peptide linkages within the data set had a ω torsion angle close to 0°, corresponding to a cis peptide bond [2].

Approximately 5% of all Xaa-Pro peptides are known to occur in the cis conformation (Xaa describes any amino acid). However, only 0.03% of Xaa-non-Pro peptides are observed in the cis conformation [4]. Cis peptides are primarily observed with proline because the trans and cis isomers of

the prolyl peptide bonds experience similar steric clashes between the neighboring side-chains. Also, the trans conformation is slightly destabilized due to steric interactions between the proline side-chain and the backbone atoms [5].

While the occurrence of Xaa-non-Pro peptide bonds is rare, there is a strong correlation between the number of Xaa-non-Pro peptide bonds detected and the resolution of the protein crystal structure. Using a nonredundant set of 571 proteins, Weiss and co-workers revealed that high-resolution protein crystal structures (<2 Å) contain twice as many Xaa-Pro and four times as many Xaa-non-Pro cis peptide bonds as medium resolution protein crystal structures (2-2.5 Å) [4]. Therefore, it is possible that cis peptide bonds are more prevalent than currently believed, but are under represented in lower resolution protein crystal structures. Unless the fit to electron density is quite poor in the trans conformation, the presence of a cis dihedral may be overlooked and the ω torsion angle is automatically and incorrectly set to 180° during refinement [6].

While trans peptide bonds are located in all types of secondary structure, cis peptide bonds are primarily found in bends and β turns [6]. More specifically, type IV β turns are most commonly found to contain cis peptide bonds. A study covering 775 protein families found that approximately 26% of all cis peptide linkages are located in type IV β

turns (Figure 1.3). The presence of a cis peptide bond in a β turn allows the peptide to easily change direction or fold back on itself. Type VIa and VIb β turns, as well as coils and extended β strand conformations, are each found to represent approximately 15% of all cis peptide bonds [2,6,7].

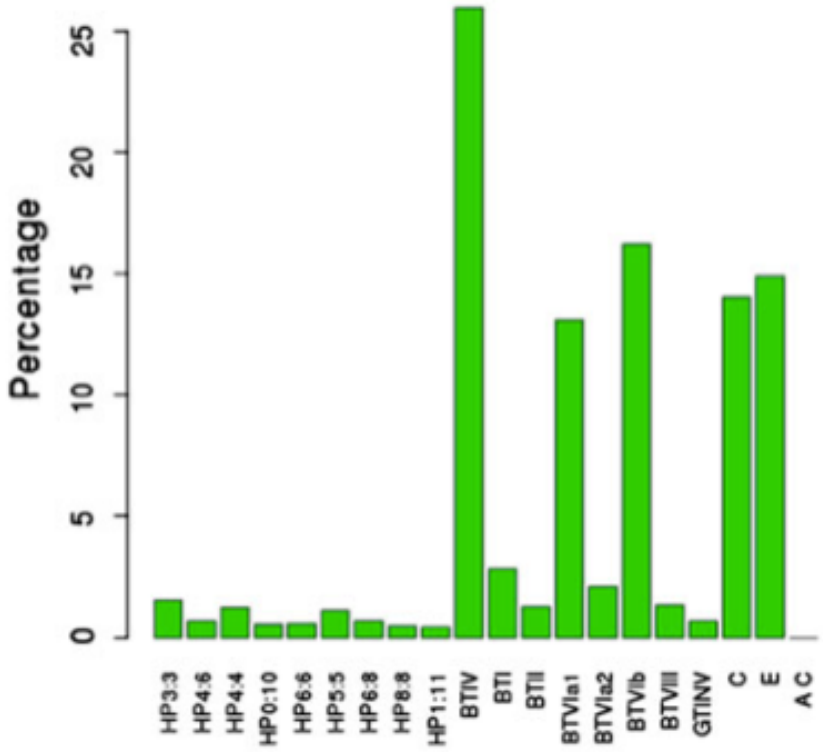

Figure 1.3 Local secondary structure preferences for cis peptide bonds. BTX represents β turns where X is the type of turn. C represents coils, E represents extended β strand conformations, and AC represents antiparallel strands. *GTINV* represents inverse γ -turns and HP X:Y represents β hairpins where X and Y represent the number of residues in the loop [2].

It has also been determined that there is a higher propensity for aromatic amino acids to be found at the first site of a prolyl cis peptide bond. This is likely due to the stabilizing π interactions, which can exist, between proline and the aromatic rings of residues such as phenylalanine, tyrosine, and tryptophan when the peptide bond is in the cis conformation. Glycine and alanine are also commonly found in the first site of a prolyl cis peptide bond, with glycine occupying the site approximately 12% of the time and alanine occupying the site approximately 9% of the time. It is believed that the presence of theses small residues reduces the steric hindrance at the site of the cis peptide bond [8]. Currently, there is no reliable statistical data on the frequency of particular amino acids to be found in non-prolyl cis peptide bonds due to their exceedingly rare occurrence and the wide variety of amino acids involved.

Occasionally, cis peptide bonds have important biological functions. For example, human cellular factor XIII zymogen has two non-prolyl cis peptide bonds. One non-prolyl cis peptide bond located near its active site and the other located near its dimerization interface [9]. Cis-trans isomerization can control protein autoinhibition, as in the case of adaptor molecule Crk, which binds to tyrosine-phosphorylated proteins. When the proline residue of the chain that links the two domains is in the cis conformation, the two domains interact intramolecularly and Crk is

autoinhibited. However, in the trans conformation, Crk exists in an active state [10]. Also, cis-trans isomerization can play a role in ion channel gating. The isomerization of a single proline residue of 5-hydroxytryptamine type 3 receptor allows the ion channel to switch between open and closed states [11]. Finally, is has been shown that trans-cis isomerization of a proline residue of brain factor-1 (BF1) controls the ability of the protein to bind to the cell membrane. In this situation, BF1 is only able to bind to the cell membrane when this proline residue is in the cis conformation [12].

Cis-trans isomerization about the rigid peptide bond of the protein backbone is a very slow reaction and significant to both the protein structure and folding pathway (Figure 1.4). The proposed activation barrier of cis-trans isomerization of a prolyl-peptide bond has been experimentally determined to be approximately 20 kcal/mol with an addition cost of 2 kcal/mol for non-prolyl peptide bonds [13]. Cis-trans prolyl isomerases are necessary to overcome this activation barrier and allow for the formation of a cis peptide bond by acting as a protein-folding chaperone. Several cis-trans prolyl isomerases, such as cyclophilin and parvulin, are known to exist. However, thus far only one isomerase has been identified to be able to catalyze the trans-cis isomerization of a non-prolyl cis peptide bond. The Hsp70 chaperone DnaK has shown trans-cis isomerase activity for alanine-Xaa dipeptides where Xaa represents

methionine, alanine, serine, glutamine, leucine, isoleucine, glycine, or lysine. This trans-cis isomerization activity was shown to be specific for non-prolyl Ala-Xaa dipeptides because Dnak was not able to catalyze the trans-cis isomerization of an Ala-Pro dipeptide [14]. Despite this work in dipeptides, there are no know non-prolyl trans-cis isomerase that catalyze the formation non-prolyl cis peptide bonds in native protein structures. However, it is possible that the isomerization of non-prolyl cis peptide bonds in native protein structures is not catalyzed by isomerases. Stabilizing interactions that occur during the folding of the overall protein structure may drive trans to cis isomerization in proteins containing non-prolyl cis peptide bonds [15].

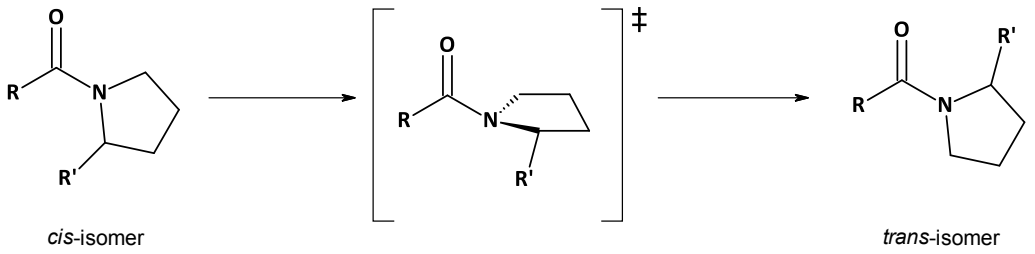

Figure 1.4 Cis-trans isomerization of a Xaa-Pro peptide bond (Where Xaa is any amino acid). Isomerization proceeds through a one-step mechanism that involves a planar transition state.

Unfolded proteins typically only contain trans peptide bonds due to the high activation barrier of trans to cis isomerization. This high activation barrier can dramatically slow down protein folding and result in the

production of folding intermediates or unfolded subspecies that fold on different pathways [7]. The unfolding of proteins containing cis peptide bonds is believed to be sequential with the majority of the protein rapidly unfolding before cis-trans isomerization takes place. The refolding of these proteins is believed to undergo rapid partial folding containing the incorrect trans isomer that is followed by slow trans to cis isomerization as the rate-limiting step. However, trans to cis isomerization must be tightly coupled to the formation of protein structure because the equilibrium constant K_{eq} = [trans]/[cis] must be decreased by several orders of magnitude by the formation of a partially folded intermediate for isomerization to take place [15].

Several studies have revealed complex folding kinetics for proteins containing cis peptide bonds. Many proteins that do not contain cis peptide bonds are found to fold rapidly via a two-step mechanism without transiently populated partially folded intermediates. However, proteins containing cis peptide bonds are found to fold via a three to four step mechanism that contains one or two slow folding steps [16]. To study the folding kinetics of proteins containing cis peptide bonds, the three cis proline residues of the protein tendmistat were mutated to alanine. Wild type tendmistat typically exhibits two rapid folding phases, however a very small population of tendmistat molecules display two slower folding

reactions that are attributed to prolyl trans-cis isomerization. This study has revealed that despite the substitution of the cis proline residues for alanine, the slow folding phases were observed in the mutant protein. This indicates that all three sites remain in the cis conformation even after mutagenesis. In an effort to attribute the slow folding phases of the mutant protein to non-prolyl trans-cis isomerization, the mutant protein was denatured with lithium chloride in anhydrous trifluoroethanol (TFE). Lithium chloride in TFE was previously shown to increase the cis peptide bond content of small peptides. This experiment revealed that increasing the concentration of lithium chloride in TFE increased the population of slow folding mutated tendmistat molecules. Therefore, it was concluded that non-prolyl trans-cis isomerization is responsible for the observed slow folding steps in mutated tendmistat [17].

1.2 Plasma PAF-AH and Atherosclerosis

Platelet activating factor (PAF) is a pro-inflammatory phospholipid that is primarily produced in cells that are involved in host defense, such as endothelial cells, monocytes, macrophages, neutrophils, and platelets. PAF is constantly produced by these cells in small quantities, but can be produced in larger amounts in response to certain stimuli, such as the uptake of thrombin by endothelial cells and macrophages undergoing

phagocytosis. PAF can be produced via either a *de novo* pathway or through a lipid-remodeling pathway. PAF levels are maintained during typical cellular function through the *de novo* pathway, in which PAF is synthesized from 1-O-alkyl-2-acetyl-sn-glycerol (AAG), 1-O-hexadecyl, and phosphocholine. Inflammatory agents activate the lipid-remodeling pathway of PAF production. Through this pathway, the fatty acid is removed from the sn-2 position of phosphatidylcholine by phospholipase A2 to produce lyso-phosphatidylcholine. An acetyl group is then attached by lyso-phosphatidylcholine acetyltransferase to generate PAF [18,19].

PAF is degraded by a family of enzymes known as PAF acetylhydrolases. These enzymes include, platelet-activating factor acetylhydrolase (PAF-AH), Platelet-activating factor acetylhydrolase 2 (PAF-AH2), and Platelet-activating factor acetylhydrolase 1b (PAF-AH1B). PAF acetylhydrolases degrade PAF by hydrolyzing the ester bond at the sn-2 position to produce the biologically inactive products lyso-PAF and acetate (Figure 1.5) [20,21].

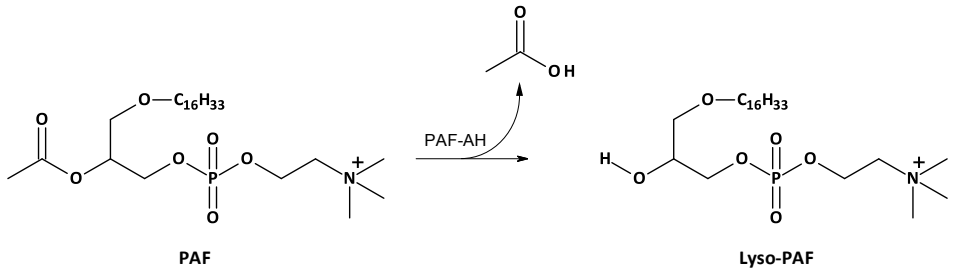

Figure 1.5 The degradation of PAF by PAF-AH. PAF-AH hydrolyses the ester bond of PAF at the sn-2 position to produce lyso-PAF and acetate. PAF-AH is a 46-kDa protein that consists of 441 amino acids.

PAF-AH is also known as lipoprotein-associated phospholipase A_2 (Lp-PLA_2) and circulates in human blood plasma associated to low density lipoproteins (LDL) and high density lipoproteins (HDL). PAF-AH functions on the lipid-aqueous interface and can therefore be considered a peripheral membrane protein (Figure 1.6). PAF-AH contains a GXSXGX motif that is characteristic of neutral lipases and serine esterases and is calcium independent [20,21]. The active site of PAF-AH contains a catalytic triad that consists of Ser-273, His-351, and Asp-296. Ser-273 is part of the conserved GXSXGX motif and is located at the N terminus of an α-helix. His-351 is also located at the N terminus of an α-helix and Asp-296 on the C-terminal end of a β-sheet. His-351 and Asp-296 are positioned nearby nucleophillic Ser-273 to allow for the activation of Ser-273 for catalysis. It is also believed that the substrates can enter the active site originating from either lipoproteins or the aqueous phase [18, 20].

Clinically, PAF-AH is known to play a role in atherosclerosis. Atherosclerosis is an inflammatory disease that is caused by the formation of plaques in the inner lining of arteries. These plaques are comprised of white blood cells, cholesterol, and triglycerides and are covered by a fibrous cap made of connective tissue. Atherosclerotic plaques are formed when monocytes are transported across the endothelial barrier into the arterial intima. From there, the monocytes are differentiated into macrophages, which express scavenger receptors that take up oxidized LDL. Oxidized LDL particles then accumulate in the cytoplasm of the macrophages and eventually convert them into foam cells. The accumulation of foam cells can then create a necrotic center of atherosclerosis. While the formation of plaques reduces the elasticity of the artery walls, in humans blood flow is typically not affected for decades because the artery muscular wall can be expanded around the location of the plaque. However, stiffening of the artery muscular wall can eventually lead to increased pulse pressure in advanced stages of disease. Atherosclerotic plaques are categorized as being either stable or unstable. Stable atherosclerotic plaques typically produce no symptoms and are primarily composed of smooth muscle cells and extracellular matrix. Unstable atherosclerotic plaques predominantly contain macrophages and foam cells and are characterized by a weak fibrous cap that is susceptible

to rupture. Importantly, rupture of the fibrous cap can lead to blood clot formation, heart attack, or stroke [22,23,24,25].

In addition to the signaling ligand PAF, PAF-AH is capable of hydrolyzing other substrates, such as oxidized phospholipids. This includes oxidized phosphatidylcholine that is produced during the oxidation of LDL. Therefore, PAF-AH was initially believed to play an anti-inflammatory role against atherosclerosis. However, PAF-AH is currently believed to aid in the formation of atherosclerotic plaques. The cleavage of oxidized phosphatidylcholine produces lysophosphatidylcholine and oxidized nonesterified fatty acids, which are proinflammatory and proapoptotic lipid mediators. The buildup of these proinflammatory lipids is believed to support atherosclerotic plaque expansion, as well as the establishment and advancement of the necrotic centers of atherosclerosis [25]. Multiple studies including over 25,000 healthy patients have detected a link between elevated levels of plasma PAF-AH and future cardiovascular events, such as heart attack, death, and acute cardiac syndromes. This link has encouraged several researchers to propose the use of plasma PAF-AH as a potential biomarker to evaluate the possibility of future cardiovascular events [26].

1.3 Non-Prolyl Cis-Peptide Bond in PAF-AH

PAF-AH has a non-prolyl cis peptide bond between Phe-72 and Asp-73 (Figure 1.6, 1.7). These residues are located in a β-hairpin type IV that extends from Ser-64 to Ser-87. The existence a non-prolyl cis peptide bond at this location serves no known purpose. Furthermore, the trans-cis isomerization may complicate the folding kinetics of PAF-AH and create a transient population of partially folded intermediates. This heterogeneity in the unfolded state of the protein may give rise to a series of slow-folding reactions that are coupled to the actual folding process. These slow reactions may dramatically slow the overall rate of protein folding and contribute to the high activation barrier of isomerization. Furthermore, protein heterogeneity caused by trans-cis isomerization may hinder the production of diffraction quality crystals. For example protein heterogeneity can lead to the formation of crystals that are too small for x-ray structural analysis, produce crystals that incorporate impurities and reduce crystalline order, or completely hinder the formation of crystals. Therefore, a protein sample must be pure with regards to protein conformation in addition to purity regarding contaminating agents [27].

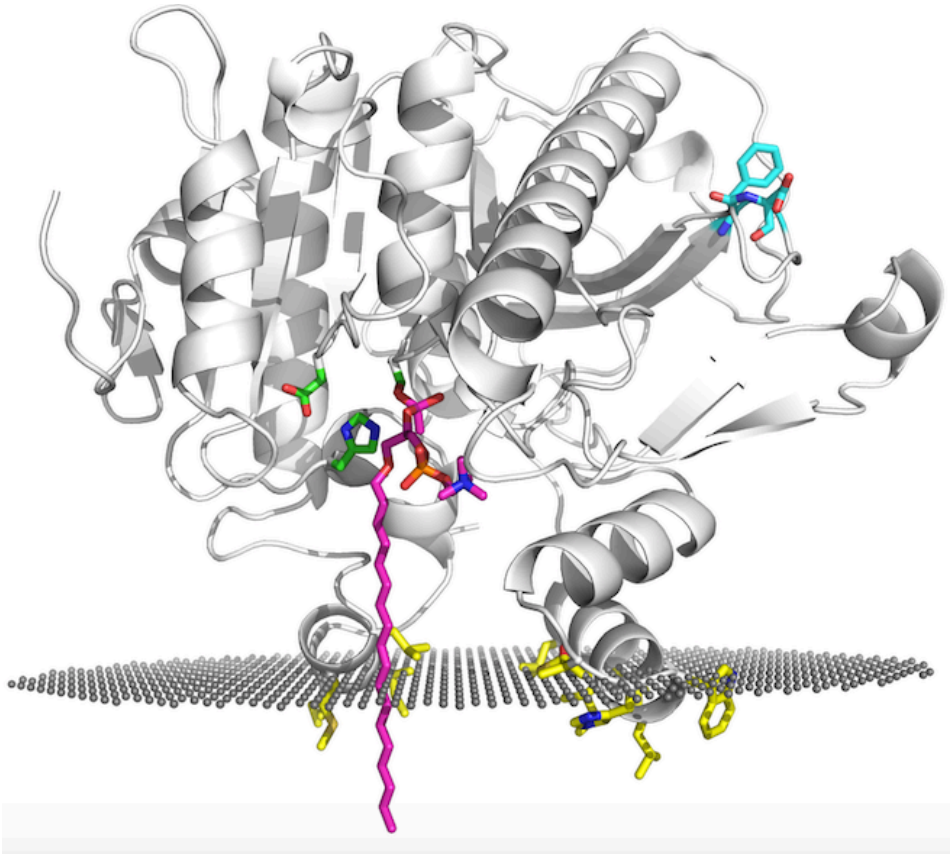

Figure 1.6 Ribbon diagram showing the predicted orientation of plasma PAF-AH on a membrane surface bound to paroxon at the active site (purple). The location of the non-prolyl cis-peptide bond is shown in blue (Phe-72, Asp-73), the location of the active site is shown in green (Ser-273, His-351, Asp-296), and the residues of the i-face are shown in yellow (His-114, Trp-115, Lys-116, Met-117, Ile-120, Lys-123, Lys-124, Ile-364, Ile-365, Met-368, Lys-369).

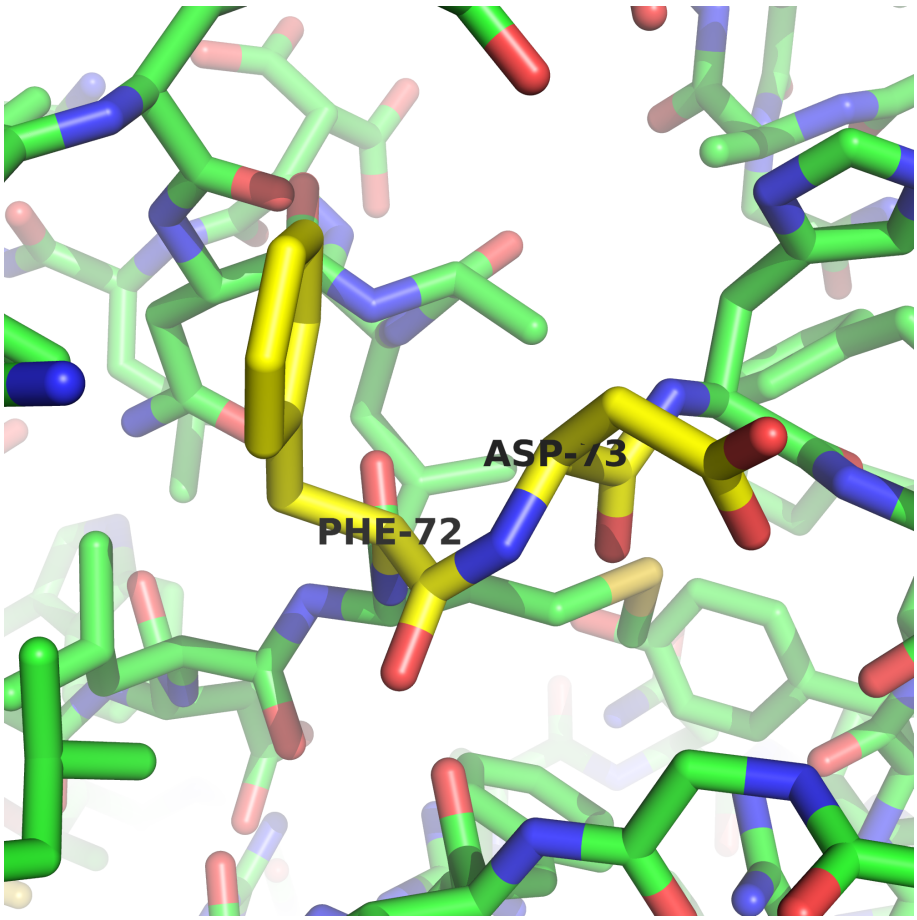

Figure 1.7 Stick diagram of plasma PAF-AH featuring Phe-72 and Asp-73 highlighted in yellow.

In an effort to create a more homogenous plasma PAF-AH protein sample and possibly increase the overall yield of pure protein, three mutations were produced at the site of the non-prolyl cis peptide bond. The first of these mutations, D73G, involved the mutagenesis of Asp-73 to glycine. The second mutation, F72GD73G, involved the mutagenesis of both Phe-72 and Asp-73 to glycine. The rationale behind both of these mutations was to reduce the size of the side chains at residues 72 and 73

in an effort to eliminate the local influence that force the formation of a cis-peptide and allow for a trans peptide bond at this site. Ideally, these mutations will create a more homogenous protein sample that will eliminate potential partially folded intermediates and facilitate protein crystallization. The third mutation, F72ED73G, involved the mutagenesis of phenylalanine-72 to glutamate and aspartate-73 to glycine. This mutation was created to mimic PAF-AH II at the site of the cis peptide bond. PAF-AH and PAF-AH II are homologous to each other with 41% sequence identity. In addition to PAF, PAH-AH II can hydrolyze a variety of phospholipid substrates and also contains a GXSXGX motif [28]. However, the crystal structure of PAF-AH II has not yet been solved and it is unknown if residues 72 and 73 are in the cis conformation in PAF-AF II. A potential consequence for this mutation is that substitution at this site for glutamate and glycine produces a trans peptide bond that would eliminate the need for trans-cis isomerization during protein folding. Subsequently, this mutation could eliminate potential partially folded intermediates and create a more homogenous protein sample.

REFERENCES

1. Craveur, P., Joseph, A. P., Poulain, P., de Brevern, A. G., Rebehmed, J. (2013) Cis-Trans Isomerization of Omega Dihedrals in Proteins. *Amino Acids*. *45,* 279-289.

2. Joseph, A. P., Srinivasan, N., de Brevern, A. G. (2012) Cis-Trans Peptide Variations in Structurally Similar Proteins. *Amino Acids*. *43,* 1369-1381.

3. Mathieu, S., Poteau, R., Trinquier, G. (2008) Estimating the "steric clash" at cis peptide bonds. *J. Phys. Chem. B. 112,* 7894-7902.

4. Weiss, M. S., Jabs, A., Hilgenfeld, R. (1998) Peptide bonds revisited. *Nat. Struct. Biol.* 5, 676.

5. Ramachandran, G. N., Mitra, A. K. (1976) An Explanation for the Rare Occurrence of Cis Peptide Units in Proteins and Polypeptides. *J. Mol. Biol*. *107,* 85-92.

6. Stewart, D. E., Sarkar, A., Wampler, J. E. (1990) Occurrence and Role of Cis Peptide Bonds in Protein Structures. *J. Mol. Biol*. *214,* 253-260.

7. Hacke, M., Gruber, T., Schilenburg, C., Balbach, J., Arnold, U. (2013) Consequences of Proline-to-Alanine Substitutions for the Stability and Refolding of Onconase. *The FEBS Journal*. *280,* 4454-4462.

8. Wu, W. J., Raleigh, D. P. (1998) Local Control of Peptide Conformation: Stabilization of Cis Proline Peptide Bonds by Aromatic Proline Interactions. *Biopolymers*. *45,* 381-394.

9. Weiss, M. S., Metzner, H. J., Hilgenfeld, R. (1998) Two Non-Proline Cis Peptide Bonds May Be Important for Factor Xiii Function. *FEBS Lett*. *423,* 291-296.

10. Sarkar, P., Saleh, T., Tzeng, S. R., Birge, R. B., Kalodimos, C. G. (2011) Structural Basis for Regulation of the Crk Signaling Protein by a Proline Switch. *Nat. Chem. Biol. 7,* 51-57.

11. Lummis, S. C., Beene, D. L., Lee, L. W., Lester, H. A., Broadhurst, R. W., Dougherty, D. A., (2005) Cis-trans Isomerization at a Proline Opens the Pore of a Neurotransmitter-Gated Ion Channel. *Nature*. *438,* 248-252.

12. Evans, T. C., Nelsestuen, G. L. (1996) Importance of Cis-Proline 22 in the Membrane-Binding Conformation of Bovine Prothrombin. *Biochemistry*. *35,* 8210-8215.

13. Scherer, G., Kramer, M., Schutkowski, M., Reimer, U., Fischer, G. (1998) Barriers to Rotation of Secondary Amide Peptide Bonds. *J. Am. Chem. Soc*. *120,* 5568-5574.

14. Schiene-Fischer, C., Habazetti, J., Schmid, F. X., Fischer, G. (2002) The hsp70 chaperone DnaK is a secondary amide peptide bond cis-trans isomerase. *Nat. Struct. Biol. 9,* 419- 424.

15. Odfrey, C., Mayr, L. M., Schmid, F. X. (1995) Non-prolyl cis-trans peptide bond isomerization as a rate-determining step in protein folding. *J. Mol. Biol. 245,* 69-78.

16. Wu, Y., Matthews, R. (2002) A cis-prolyl peptide bond isomerization dominates the folding of the alpha subunit of Trp synthase, a TIM barrel protein. *J. Mol. Biol*. *322,* 7-13.

17. Pappenberger, G., Aygun, H., Engels, J., Reimer, U., Fischer, G., Kiefhaber, T. (2001) Nonprolyl cis peptide bonds in unfolded proteins cause complex folding kinetics. *Nat. Struct. Biol. 8,* 452-458.

18. Tjoelker, L. W., Eberhardt, C., Unger, H., Zimmerman, G. A., McIntyre, T. M., Stafforini, D. M., Prescott, S. M., Gray, P. W. (1995) Plasma platelet-activating factor acetylhydrolase is a secreted phospholipase A2 with a catalytic triad. *J. Biol. Chem*. *270,* 25481-25487.

19. Prescott, S. M., Zimmerman, G. A., Stafforini, D. M., McIntyre, T. M. (2000) Platelet-activating factor and related lipid mediators. *Annu. Rev Biochem*. *69,* 419-445.

20. Samanata, U., Bahnson, B. J. (2008) Crystal structure of human plasma platelet-activating factor acetylhydrolase: structural implication to lipoprotein binding and catalysis. *J. Biol. Chem*. *283,* 31617-31624.

21. Stafforini, D. M., Tjoelker, L. W., McCormick, S., Vaitkus, D., McIntyre, T. M., Gray, P. W., Young, S. G., Prescott, S. M. (1999) Molecular basis of the interaction between plasma platelet-activating factor acetylhydrolase and low density lipoprotein. *J. Biol. Chem*. *274,* 7018-7024.

22. Srinivasan, P., Bahnson, B. J. (2010) Molecular model of plasma PAF acetylhydrolase-lipoprotein association: insights from the structure. *Pharmaceuticals*. *3,* 541-557.

23. Ross, R. (1999) Atherosclerosis — An Inflammatory Disease. *N. Engl. J. Med. 340,* 115-126.

24. Finn, A., Nakana, M., Narula, J., Kolodgie, F., Virmani, R. (2010) Concept of vulnerable/unstable plaque. *Arterioscler. Thromb. Vasc. Biol. 30,* 1282-1292.

25. Wilensky, R. L., Macphee, C. H. (2009) Lipoprotein-associated phospholipase A(2) and atherosclerosis. *Curr Opin Lipidol. 20,* 415-420.

26. Anderson, J. L. (2008) Lipoprotein-associated phospholipase A2: an independent predictor of coronary artery disease events in primary and secondary prevention. *Am. J. Cardiol. 101,* 23-33.

27. Benvenuti, M., Mangani, S. (2007) Crystallization of soluble proteins in vapor diffusion for x-ray crystallography. *Nature Protocols*. *2,* 1633-1651.

28. Rice S. Q. J., Southan, C., Boyd, H. F., Terrett, J. A., Macphee, C. H., Moores, K., Gloger, I. S., Tew, D. G. (1998) Expression, purification and characterization of a human serine-dependent phospholipase A2 with high specificity for oxidized phospholipids and platelet activating factor. *Biochem J. 330,* 1309-1315.

Chapter 2

MOLECULAR CLONING AND MUTAGENESIS OF PAF-AH

2.1 Introduction

Human plasma PAF-AH was initially purified from human plasma in 1986 by Stafforini et al[1]. Given that plasma PAF-AH is associated with LDL in vivo and is hydrophobic nature, the detergent Tween 20 was used to solubilize LDL prior to chromatographic purification steps[1]. The human plasma PAF-AH gene was first cloned by Tjoelker et al. in 1995[2]. This was performed using a cDNA library that was produced from mRNA from monocyte-derived macrophages, which was then screened using polymerase chain reaction (PCR) and hybridization for the N-terminal sequence (IQVLMAAASFGQTKIP) of the purified protein[2].

Molecular cloning for this work was performed using a truncated human plasma PAF-AH construct (Δ PAF-AH) that spans amino acid residues 49-423. This construct contains both a C-terminal and N-terminal truncation and was produced by Dr. Prabhavathi Srinivasan from the

Bahnson lab. This construct was initially produced for protein crystallization screenings. Δ PAF-AH lacks 8 non-native amino acids at the N-terminus that are present in the parent construct which were believed to hinder crystallization. In addition, Δ PAF-AH also lacks 18 amino acids at the C-terminus, which were removed to aid in protein solubility[3] and which are known to be non-essential for proper folding and full enzyme activity.

Δ PAF-AH was initially cloned into a bacterial expression vector, pGEX-4T3 vector (GE Life Sciences), for expression as a glutathione S-transferase (GST) fusion protein with a molecular weight of 69 kDa. GST is cleaved from the GST-PAF-AH fusion via a thrombin cleavage site using thrombin protease. However, thrombin protease has been reported to cleave non-specifically at secondary sites within some over expressed proteins. This non-specific cleavage of recombinant proteins can generate heterogeneous protein samples that can impair protein structural studies such as NMR spectroscopy and X-ray crystallography[4]. For this reason, Δ PAF-AH was subcloned into pGEX-6P1 (GE Life Sciences) to allow for the fusion protein to be cleaved with PreScission Protease. Upon removal of the GST tag using PreScission Protease, purified recombinant Δ PAF-AH has a molecular weight of 43 kDa. Δ PAF-AH will be referred to as PAF-AH throughout this work.

2.2 Molecular Cloning of PAF-AH

PAF-AH, in the vector pGEX-4T3, was amplified by PCR using the following primers and PCR parameters (Figure 2.1):

Forward: 5' AAAAAAGGATCCTCCTTTGGCCAAACT 3'

Reverse: 5' AAAAAACAGCTGGTTAATGTTGGTCCCT 3'

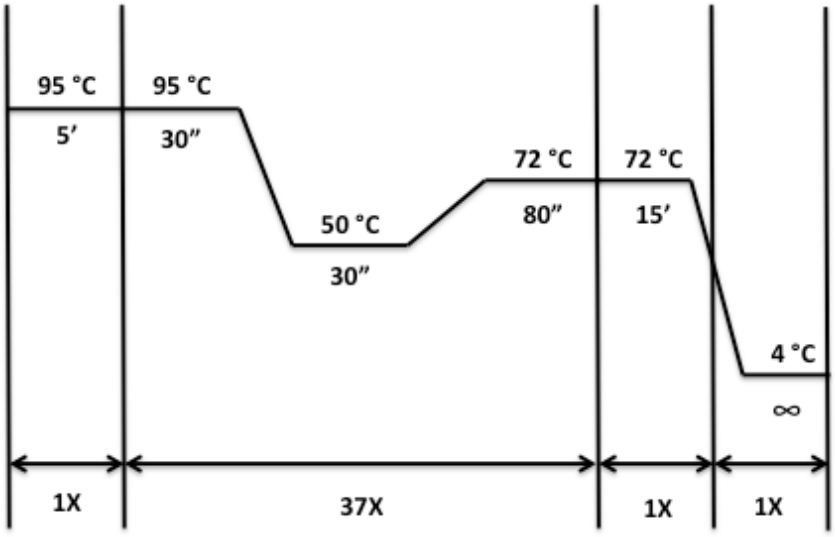

Figure 2.1 The PCR cycle parameters used for the amplification of PAF-AH insert in pGEX-4T3 vector.

The resulting PCR product was purified using QIAquick PCR Purification Kit (Qiagen). A restriction enzyme double digest using *Bam*HI and *Sal*I was performed on amplified PAF-AH insert and pGEX-6P1 vector. PAF-AH insert was ligated into pGEX-6P1 vector and transformed

into DH5α chemically competent cells. Cells from individual colonies were grown in 5 mL of culture and purified using QIAprep Spin Miniprep Kit (Qiagen).

2.3 Mutagenesis of PAF-AH

2.3.1 D73G

The 73rd residue of PAF-AH was mutated from aspartate to glycine through site directed mutagenesis. The PCR procedure was performed using 1 μL plasmid DNA (30 ng/μL), 1.5 μL forward primer, 1.5 μL reverse primer, 2 μL dNTP mix, 5 μL 10x reaction buffer, and 1 μL pfu Ultra DNA polymerase. Asp-73 was mutated to glycine using the following primers:

Forward: 5' CAGACTTAATGTTTGGTCACACTAATAAGGGC 3'

Reverse: 5' GCCCTTATTAGTGTGACCAAACATTAAGTCTG 3'

Gradient PCR was performed to determine the optimal annealing temperature for this set of mutagenic primers. The annealing temperatures of this gradient were selected to be lower than the Tm of the primer set

(69.7 °C) and comprised of annealing temperatures ranging from 50-60 °C. A 0.8% agarose gel was run to confirm successful mutagenesis and determine the ideal annealing temperature. The optimal annealing temperature was shown to be 50 °C and Asp-73 was mutated to glycine using the following PCR parameters (Figure 2.2):

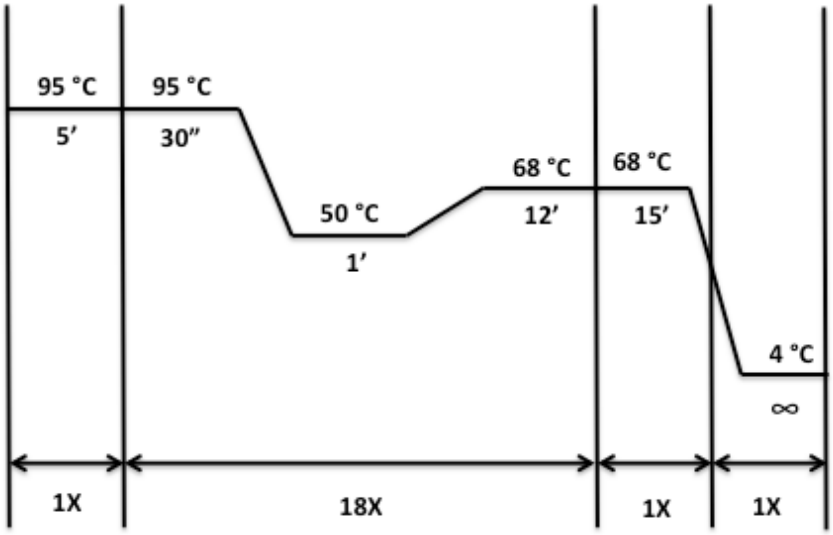

Figure 2.2 Optimal PCR cycle parameters to mutate the 73rd residue of PAF-AH from aspartate to glycine.

The mutagenic product was digested with DPN1 and transformed into DH5 α and BL21 chemically competent cells. Clones were grown in 5 mL of culture, purified using QIAprep Spin Miniprep Kit (Qiagen), and sent out for DNA sequencing (Genewiz; South Plainfield, NJ).

2.3.2 F72G/D73G

D73G in pGEX-6P1 was used as a plasmid DNA template to mutate the 72nd residue of PAF-AH from phenylalanine to glycine through site directed mutagenesis. The PCR procedure was performed using 1 μL plasmid DNA (30ng/μL), 1.5 μL forward primer, 1.5 μL reverse primer, 2 μL dNTP mix, 5 μL 10x reaction buffer, and 1 μL pfu Ultra DNA polymerase. Phe-72 was mutated to glycine using the following primers:

Forward: 5' GGTTGTACAGACTTAATGGGTGGTCACACTAATAAGG 3'

Reverse: 5' CCTTATTAGTGTGACCACCCATTAAGTCTGTACAACC 3'

Gradient PCR was performed to determine the optimal annealing temperature for this set of mutagenic primers. The annealing temperatures of this gradient were selected to be lower than the Tm of the primer set (73.0 °C) and comprised of annealing temperatures ranging from 55-65 °C. The optimal annealing temperature was shown to be 60 °C and Phe-72 was mutated to glycine using the following PCR parameters (Figure 2.3):

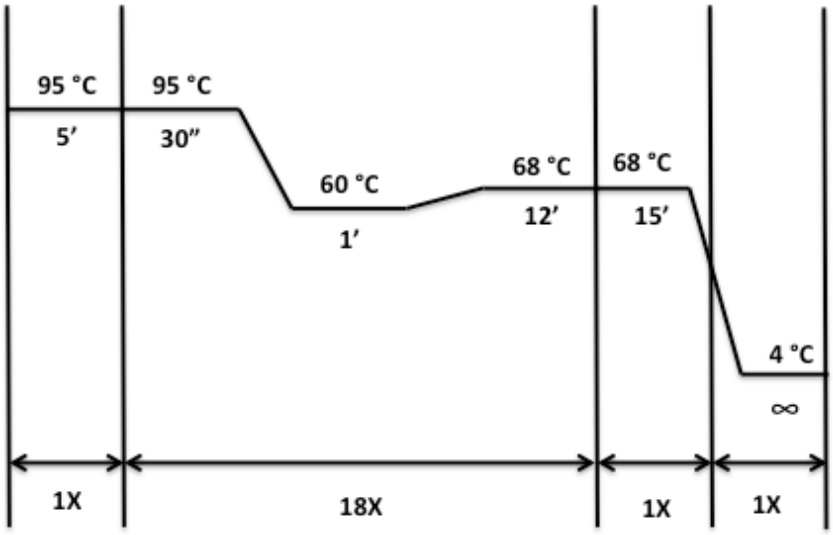

Figure 2.3 Optimal PCR cycle parameters to mutate the 72nd residue of D73G from phenylalanine to glycine.

The mutagenic product was digested with DPN1 and transformed into DH5α and BL21 chemically competent cells. Clones were grown in 5 mL of culture, purified using QIAprep Spin Miniprep Kit (Qiagen), and sent out for DNA sequencing (Genewiz; South Plainfield, NJ).

2.3.3 F72E/D73G

D73G in pGEX-6P1 was used as a plasmid DNA template to mutate the 72nd residue of PAF-AH from phenylalanine to glutamate through site directed mutagenesis. The PCR procedure was performed using 1 μL plasmid DNA (30ng/μL), 1.5 μL forward primer, 1.5 μL reverse primer, 2 μL dNTP mix, 5 μL 10x reaction buffer, and 1 μL pfu

Ultra DNA polymerase. Phe-72 was mutated to glutamate using the following primers:

Forward: 5’ GTTGGTTGTACAGACTTAATGGAAGGTCACACTAA TAAGGGCAC 3’

Reverse: 5’ GTGCCCTTATTAGTGTGACCTTCCATTAAGTCTGT ACAACCAAC 3’

Gradient PCR was performed to determine the optimal annealing temperature for this set of mutagenic primers. The annealing temperatures of this gradient were selected to be lower than the Tm of the primer set (77.3 °C) and comprised of annealing temperatures ranging from 60-70 °C. The optimal annealing temperature was shown to be 65 °C and Phe-72 was mutated to glutamate using the following PCR parameters (Figure 2.4):

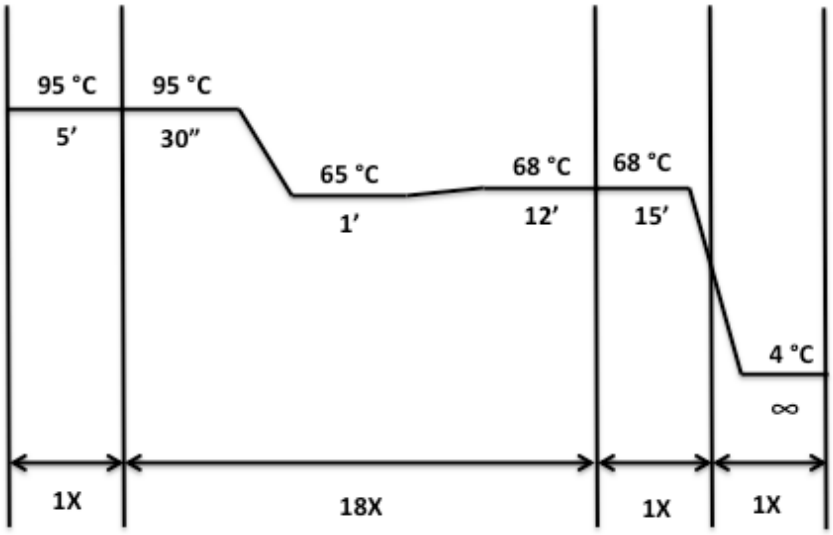

Figure 2.4 Optimal PCR cycle parameters to mutate the 72rd residue of D73G from phenylalanine to glutamate.

The mutagenic product was digested with DPN1 and transformed into DH5α and BL21 chemically competent cells. Clones were grown in 5 mL of culture, purified using QIAprep Spin Miniprep Kit (Qiagen), and sent out for DNA sequencing (Genewiz; South Plainfield, NJ).

2.3.4 DNA Sequencing Results

The production of mutant constructs D73G, F72G/D73G, and F73E/D73G were confirmed through DNA sequencing. These sequencing results were then used to perform a sequence alignment between the mutant constructs and PAF-AH (Figure 2.5) using Culstal Omega software.

Figure 2.5 DNA sequence alignment between D73G, F72G/D73G, F73E/D73G, and PAF-AH showing mutation at Phe-72 and Asp-73. Affected residues are boxed to show mutation

REFERENCES

1. Stafforini, D. M., Prescott, S. M., McIntyre, T. M. (1987) Human plasma platelet-activating factor acetylhydrolase. Purification and properties. *J. Biol. Chem***.** *262,* 4223-4230.

2. Tjoelker, L. W., Wilder, C., Eberhardt, C., Stafforimi, D. M., Dietsch, G., Schimpf, B., Hooper, S., Trong, H. L., Cousens, L. S., Zimmerman, G. A., Yamada, Y., McIntyre, T. M., Pescott, S. M., Gray, P. W. (1995) Anti-inflammatory properties of a platelet-activating factor acetylhydrolase. *Nature*. *374***,** 549-553.

3. Srinivasan, P., Bahnson, B. J. (2010) Molecular model of plasma PAF acetylhydrolase-lipoprotein association: insights from the structure. *Pharmaceuticals*. *3,* 541-557.

4. Rajalingam, D., Kathir, K. M., Ananthamurthy. K., Adams. P. D., Kumar, T. K. S. (2008) A method for the prevention of thrombin-induced degradation of recombinant proteins. *Anal Biochem*. *375,* 361-363.

Chapter 3

EXPRESSION AND PURIFICATION OF CIS-PEPTIDE BOND MUTANTS IN PAF-AH

3.1 Introduction

PAF-AH and all cis-peptide bond mutants were expressed in *E. coli* (strain BL21) and induced using isopropyl β-D-1-thiogalactopyranoside (IPTG). Each construct was then purified using a Glutathione Sepharose column followed by cleavage with PreScission Protease to remove the GST tag. In most cases, Q-Sepharose anion exchange chromatography was also used to further enhance the purity of the protein sample for crystallization trials.

The isoelectric point (pI) of each PAF-AH construct was calculated using ExPASy Compute pI tool. The predicted pI of PAF-AH and mutant construct F72ED73G was calculated to be 6.68 (Table 3.1). Therefore, to ensure a net negative charge of the protein and solubility, a

pH 7.8 buffering system was used for all purification steps. The predicted pI for mutant constructs D73G and F72GD73G was calculated to be 6.95 and a pH 8.1 buffering system was used for all purification steps.

Table 3.1: Predicted pI of PAF-AH and mutated ΔPAF-AH constructs

PAF-AH Construct	Predicted pI
PAF-AH	6.68
D73G	6.95
F72G/D73G	6.95
F73E/D73G	6.68

3.2 Protein Expression

BL21 cells were grown from a glycerol stock overnight at 37 °C in 200 mL of Luria-Bertani (LB) media with 0.1 mg/mL ampicillin. A 10 mL aliquot of overnight culture was grown in 1 L of LB medium with 0.1 mg/ml ampicillin at 37 °C until OD_{600}= 0.8 (5 h). Expression was induced with 1 mM IPTG and was left to shake overnight at 18 °C. Cell culture was centrifuged at 8,000 rpm for 8 min until the cells were pelleted. Pelleted cells were stored at -80 °C for later use.

3.3 Protein Affinity Chromatography

Pelleted cells were thawed and resuspended in lysis buffer composed of 50 mM tris base, 100 mM NaCl, 5 mM dithiothreitol (DTT), 1 mM pepstatin, and 0.1 mM lysozyme at pH 7.8 or pH 8.1 depending on the construct being purified. Cells were lysed through two rounds of sonication at 2 min each. 0.1% Triton x100 was added and lysed cells were rocked at 4 °C for 30 min. The cell lysate was centrifuged at 12,000 rpm for 20 min. The supernatant was combined with 10 mM ATP and 20 mM $MgCl_2$, rocked for 20 min at room temperature, and centrifuged again at 12,000 rpm for 20 min. A Glutathione Sepharose column was used in affinity chromatography to purify PAF-AH and its mutants, all containing a Glutathione *S*-transferase (GST) tag. The GST column was equilibrated using a wash buffer containing 50 mM tris base, 100 mM NaCl, 1 mM DTT, 5mM ATP 20 mM $MgCl_2$, and 0.1% Triton x100 at pH 7.8/ pH 8.1. The cell lysate was loaded onto the column and incubated for 1 h at 4 °C. After incubation, the flow through was drained and the column was washed with 400 mL of the wash buffer used to equilibrate the column. 10 mL of wash buffer was left on the column and incubated overnight at 4 °C with 1 mL of PreScission Protease to cleave the GST-tag from the fusion protein. After incubation, cleaved protein was drained from the column

and stored at 4 °C to be further purified through Q-Sepharose anion exchange chromatography. PreScission Protease was removed using an elution buffer containing 50 mM tris base, 100 mM NaCl, 1 mM EDTA, 1 mM DTT, 25 mM reduced glutathione, and 0.1% Triton x100 at pH 7.8/ pH 8.1.

3.4 Q-Sepharose Anion Exchange Chromatography

Protein sample purified through affinity chromatography was dialyzed into 4 L of running buffer containing 50 mM tris base, 1 mM EDTA, 20 mM NaCl, 1 mM DTT, and 0.005% Triton x100 at pH 7.8/ pH 8.1. A Q-Sepharose anion exchange FPLC column was equilibrated by washing with 15 mL of water, followed by elution buffer containing 50 mM Tris, 1 mM EDTA, 750 mM NaCl, 1 mM DTT, and 0.005% Triton x100 at pH 7.8/pH 8.1. Protein sample was loaded onto the Q-Sepharose column at a rate of 1 mL/min. An hour-long linear gradient of elution buffer was run with fractions being collected as spikes in UV were seen. Fractions containing pure protein were concentrated to 0.5 mL and dialyzed into 50 mM tris buffer at pH 7.8/ pH 8.1.

3.5 Purification of Prescisison Protease

BL21 cells containing PreScission Protease in pGEX-6P1 were grown from a glycerol stock overnight at 37 °C in 200 mL of LB medium with 0.1 mg/mL ampicillin. A 10 mL aliquot of overnight culture was grown in 1L of LB medium with 0.1 mg/ml ampicillin at 37 °C until OD_{600}= 0.8 (~5 h). Expression was induced with 1mM IPTG and was left to shake overnight at 18 °C. Cell culture was centrifuged at 8,000 rpm for 8 min until the cells were pelleted. Pelleted cells were stored at -80 °C for later use. Pelleted cells were thawed and resuspended in a buffer composed of 50mM tris base, 150 mM NaCl, 2 mM DTT at pH 8. Cells were lysed through two rounds of sonication at 2 min each. The cell lysate was centrifuged twice at 11,000 rpm for 20 min each. The cell lysate was loaded onto a Glutathione Sepharose column and incubated for 1 h at 4 °C. After incubation, the flow through was drained and the column was washed with 500 mL of the resuspension buffer. PreScission Protease was eluted from the column with 15 mL of elution buffer containing 50 mM Tris, 150 mM NaCl, 2 mM DTT, and 10 mM reduced glutathione and pH 8. Eluted PreScission protease was dialyzed into 10 mM Tris, 150 mM NaCl, and 2 mM DTT, and then stored at -80 °C in 1 mL aliquots.

3.6 BCA Assay

A BCA protein assay was performed to determine the concentration of pure protein (Pierce). Bovine serum albumin (BSA) standards were prepared ranging from 2 mg/mL to 0.125 mg/mL BSA. The BCA working reagent was prepared by mixing 50 parts of BCA Reagent A with 1 part of BCA Reagent B. BSA standards and protein samples were incubated with 1 mL of BCA working reagent each at 37 °C for 30 min. The absorbance of standards and protein samples was read at 562 nm. A standard curve was prepared by plotting the absorbance at 562 nm for each BSA standard against its concentration in mg/mL. The standard curve then used to determine the concentration of the unknown protein samples.

3.7 PNPA Activity Assay

Enzyme activity of all PAF-AH constructs was determined using p-nitrophenyl acetate (PNPA) as a substrate (Figure 3.1). The assay was performed in a 1 mL reaction volume containing 50 mM Tris at pH 7.5 and a 500x dilution of enzyme. The hydrolysis of PNPA by PAF-AH to form p-nitrophenoxide and acetate was initiated through the addition of 5 mM PNPA and the increase in absorbance at 405 nm was used to determine enzyme activity. The molar extinction coefficient of p-nitrophenoxide was

experimentally determined to accurately calculate enzyme specific activity. A calibration curve was prepared using known concentrations of p-nitrophenoxide ranging from 0.09 mM to 0.01 mM. The molar extinction coefficient of p-nitrophenoxide was determined to be 14,370 $M^{-1}cm^{-1}$ through calculating the slope of the calibration curve.

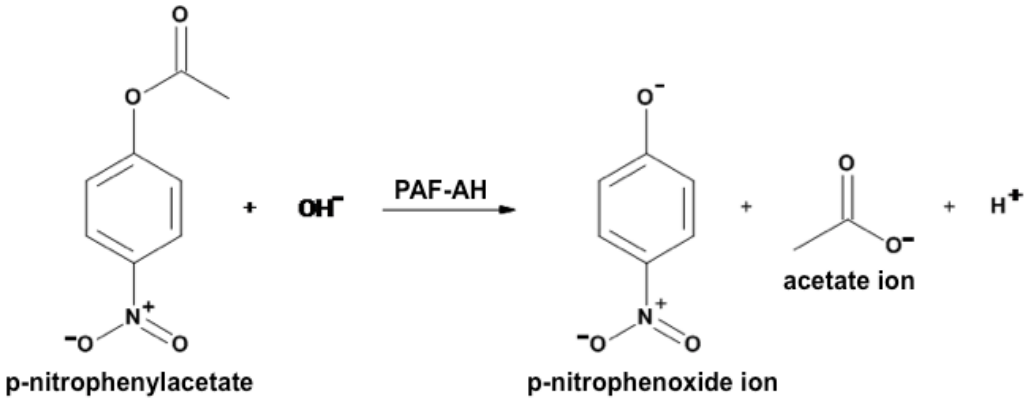

Figure 3.1 The hydrolysis of PNPA by PAF-AH to produce p-nitrophenoxide and acetate.

3.8 Results and Discussion

3.8.1 Expression and Purification of Recombinant PAF-AH and Cis-Peptide Bond Mutants

PAF-AH and all cis-peptide bond mutants were expressed in *E. coli* (strain BL21). An expression trial was preformed using varying

concentrations of IPTG, ranging from 2.5 mM to 0.1 mM IPTG. SDS-PAGE analysis was performed on whole cells obtained before and after induction with IPTG and lysed with SDS-PAGE sample buffer to access the relative quantities of expressed fusion protein. This analysis indicated that there was no relative increase in expressed protein when induction is preformed at 1 mM IPTG and greater. Therefore, 1 mM IPTG was used for all expression studies of PAF-AH and all cis-bond mutants.

PAF-AH, D73G, F72G/D73G, and F72E/D73G were expressed simultaneously in BL21 cells and induced with 1 mM IPTG after 5 h of growth. SDS-PAGE analysis was performed on whole cells obtained before and after induction with IPTG and lysed with SDS-PAGE sample buffer to visualize the relative quantities of expressed fusion protein (Figure 3.2). Through this analysis, it was shown that mutant constructs D73G and F72G/D73G express greater quantities of GST-PAF-AH fusion protein when compared to PAF-AH. This could be seen through the presence of a much darker band in lanes corresponding to induced D73G and F72G/D73G at the expected molecular weight of GST-PAF-AH fusion protein (69 kDa) when compared to PAF-AH. This analysis also shows the mutant construct F72E/D73G produces similar quantities of GST-PAF-AH fusion protein when compared to PAF-AH and much lower quantities of GST-PAF-AH fusion protein when compared to mutant constructs D73G

and F72G/D73G. From these results, it can be inferred that substitution of Phe-72 and Asp-73 for glycine residues increases the quantity protein produced in expression.

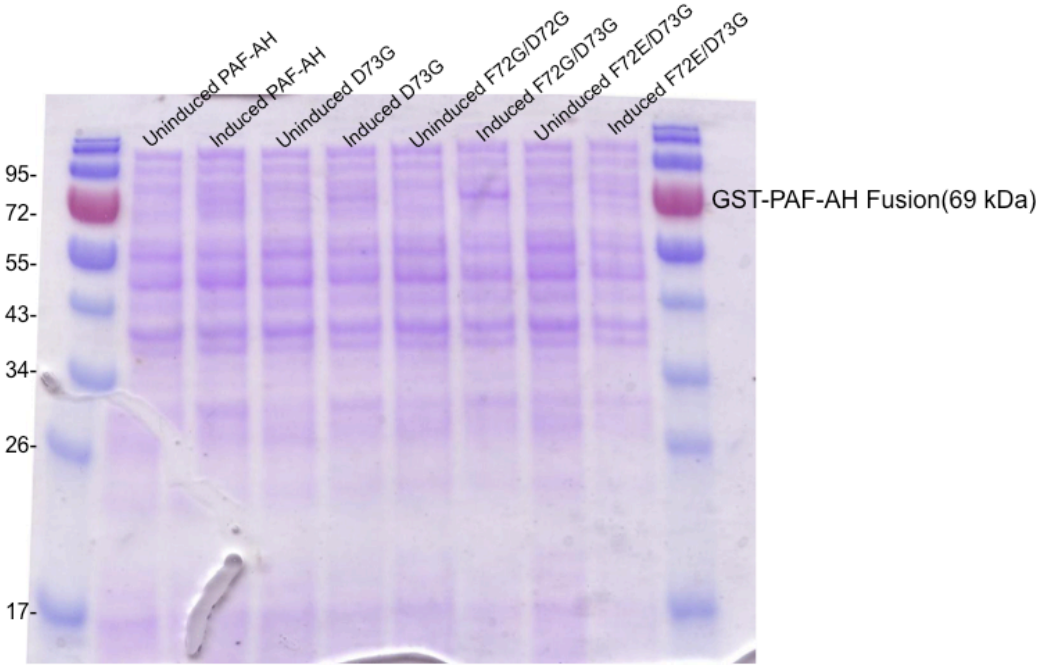

Figure 3.2 SDS PAGE analysis of whole cell expression of PAF-AH, D73G, F72GD73G, and F72ED73G before and after induction with 1 mM IPTG. Molecular weight of GST-PAFAH fusion protein is 69 kDa.

Mutant constructs D73G and F72GD73G were purified using a pH 8.1 buffering system in accordance with their predicted pI of 6.95. D73G was purified using a Glutathione Sepharose column, yielding 2.47 mg of recombinant protein per liter of cell culture (Figure 3.3). The yield of all purified PAF-AH constructs was determined through BCA assay.

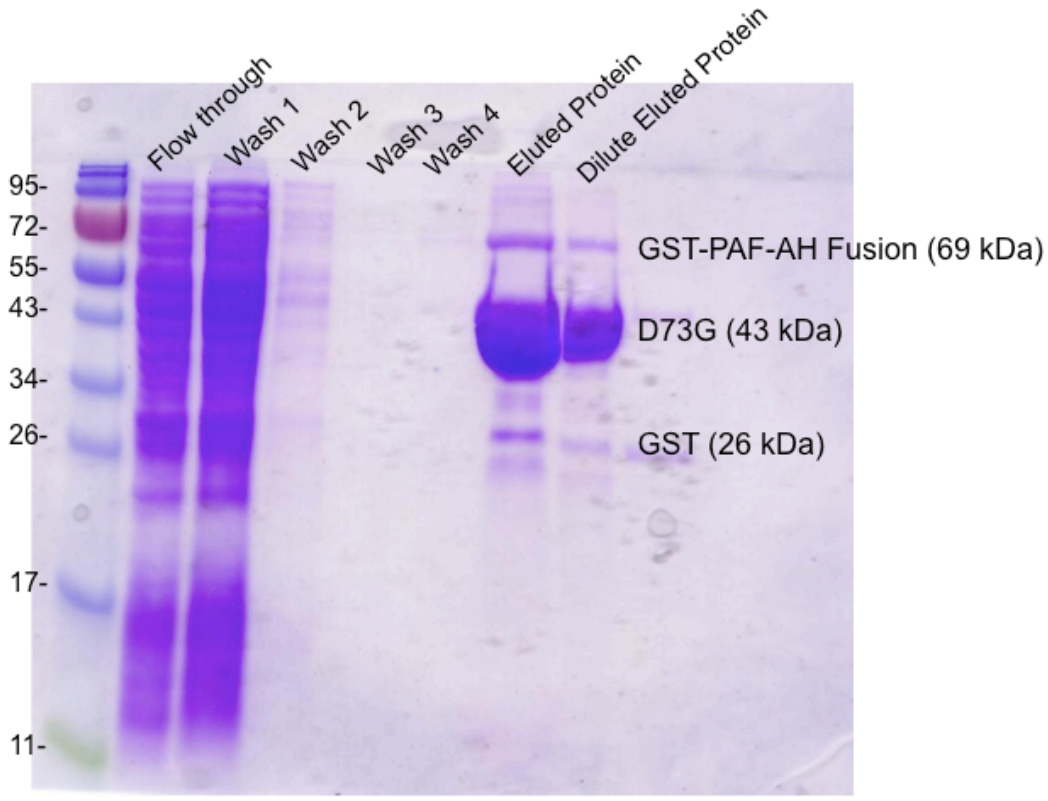

Figure 3.3 SDS Page analysis of D73G concentrated to 1 mL after purification using a glutathione Sepharose column, yielding 2.47 mg of pure protein per liter of cell culture at approximately 81% purity.

The purity of the resulting protein SDS PAGE sample was quantitated using ImageJ software and was found to be approximately 81% pure. This degree of purity is unsuitable for crystallization trials and therefore Q-Sepharose anion exchange chromatography was utilized to further enhance the purity of the protein sample. The purity of the protein sample after Q-Sepharose anion exchange chromatography was found to be approximately 96% pure (Figure 3.4). However, this process resulted in a greatly reduced yield of 1.31 mg of pure protein per liter of cell culture.

Protein product may have been lost in the protein-loading phase of Q-Sepharose anion exchange chromatography or when the sample was concentrated down to 0.5 mL. This protein sample was further concentrated to approximately 6.5 mg/mL for initial crystallization trials using Hampton Research Crystal Screens 1 and 2. However, no crystals were produced from these screens.

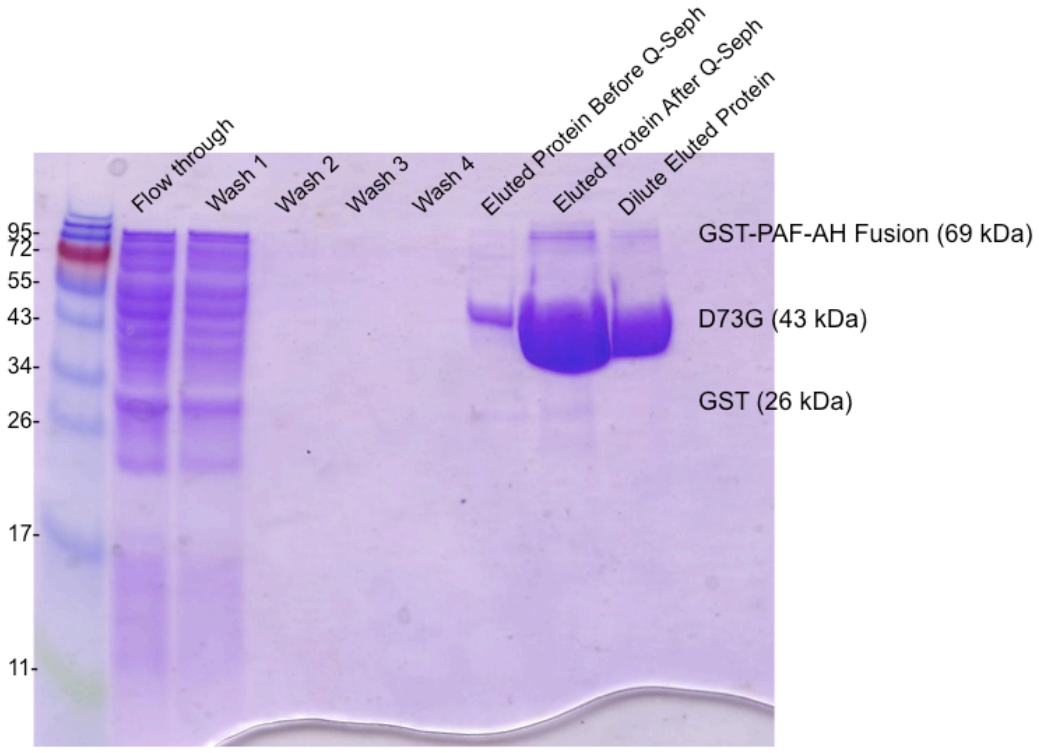

Figure 3.4 SDS PAGE analysis of purified D73G concentrated to 0.5 mL after Q-sepharose anion exchange chromatography, yielding 1.31 mg of pure protein per liter of cell culture at approximately 96% purity.

F72G/D73G was purified using a glutathione sepharose column, yielding 2.81 mg of recombinant protein per liter of cell culture (Figure 3.5).

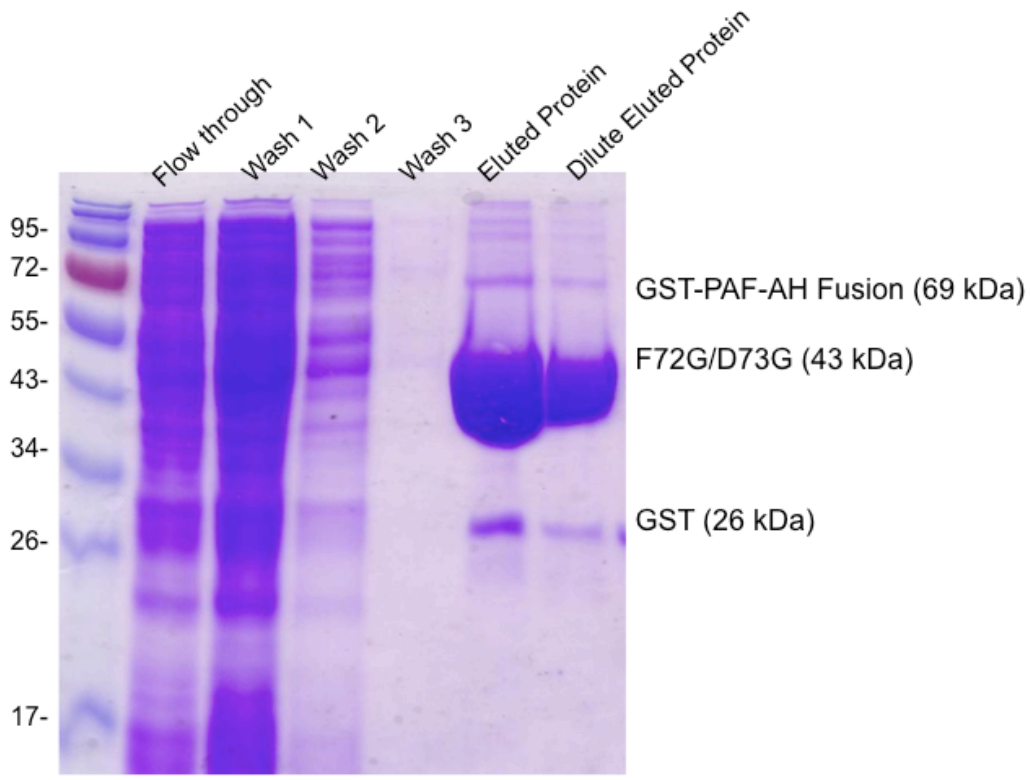

Figure 3.5 SDS Page analysis of F72G/D73G concentrated to 1 mL after purification using a glutathione sepharose column, yielding 2.81mg of pure protein per liter of cell culture at approximately 84% purity.

The purity of the resulting protein SDS PAGE sample was quantitated using ImageJ software and was found to be approximately 84% pure. This degree of purity is unsuitable for crystallization trials and therefore Q-sepharose anion exchange chromatography was utilized to

further enhance the purity of the protein sample. The purity of the protein sample after Q-sepharose anion exchange chromatography was found to be approximately 92% pure with a final yield of 2.49 mg of protein per liter of cell culture (Figure 3.6).

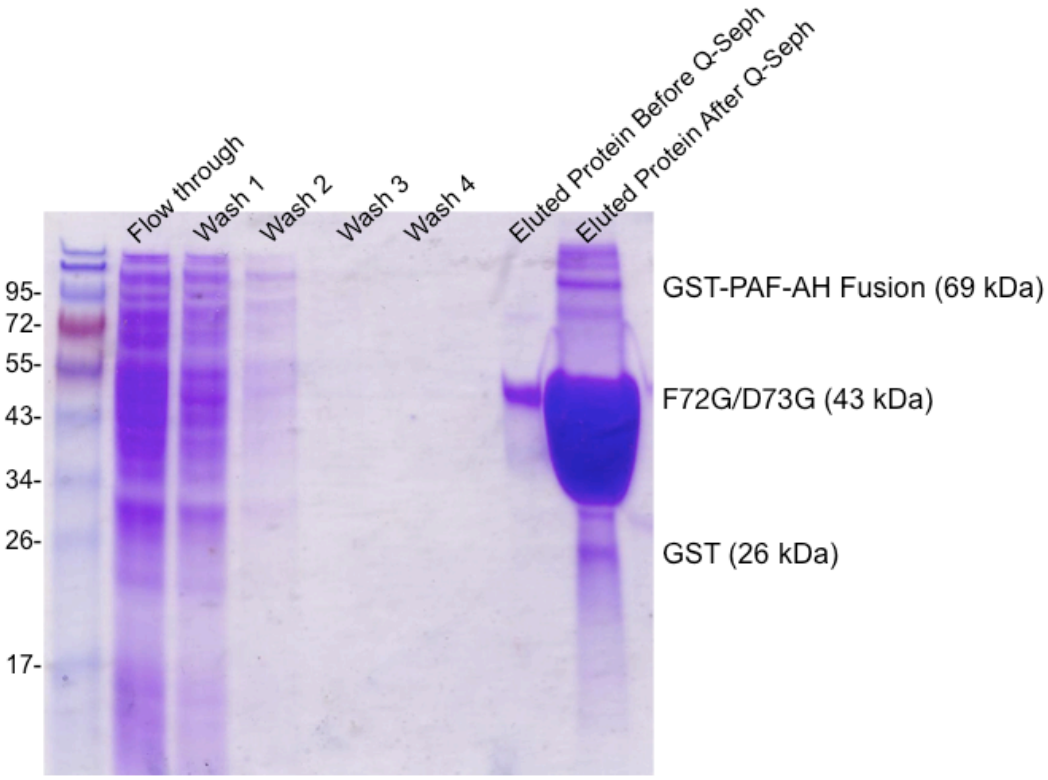

Figure 3.6 SDS PAGE analysis of purified F72G/D73G concentrated to 0.5 mL after Q-sepharose anion exchange chromatography, yielding 2.49 mg of pure protein per liter of cell culture at approximately 92% purity.

Constructs F72E/D73G and PAF-AH were purified using a pH 7.8 buffering system in accordance with their predicted pI of 6.68. F72E/D73G was purified using a glutathione sepharose column followed by

Q-sepharose anion exchange chromatography (Figure 3.7). The purity of the resulting protein sample was found to be approximately 91% pure with a final yield of 1.07 mg of protein per liter of cell culture.

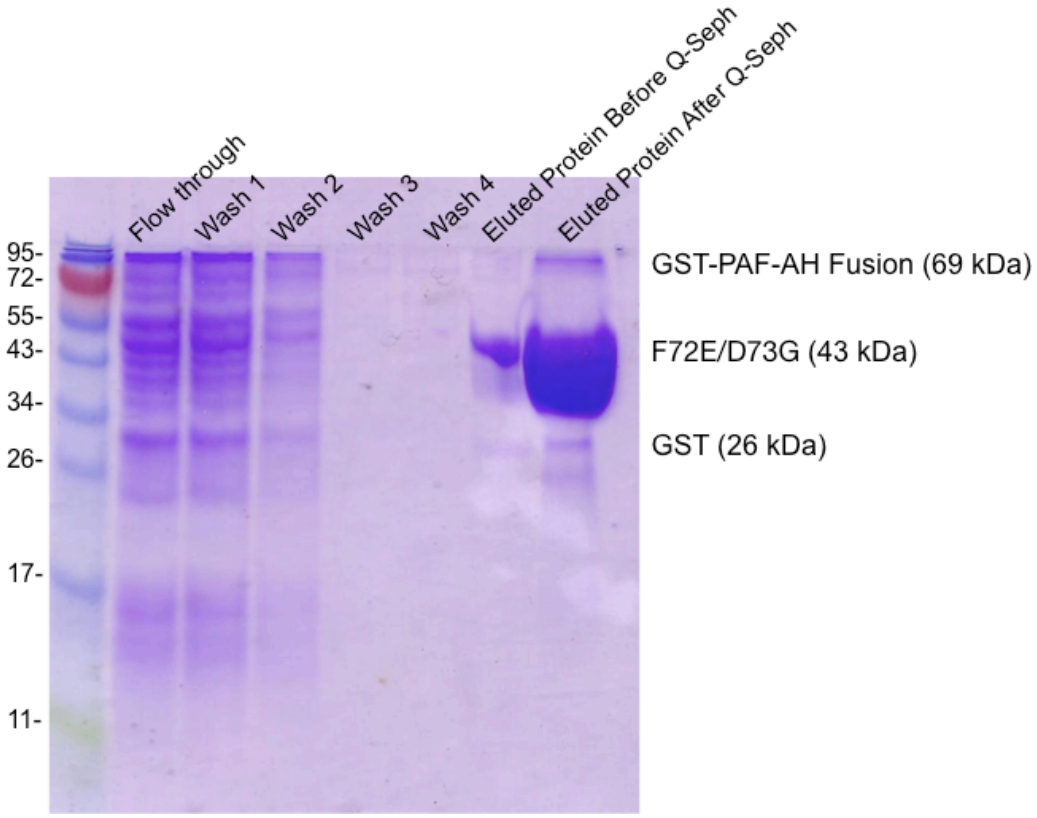

Figure 3.7 SDS Page analysis of F72E/D73G after purification after Q-sepharose anion exchange chromatography, yielding 1.07mg of pure protein per liter of cell culture at approximately 91% purity.

PAF-AH was purified using a glutathione sepharose column, yielding 0.99 mg of protein per liter of cell culture (Figure 3.8). The purity of the resulting protein SDS PAGE sample was quantitated using ImageJ

software and was found to be approximately 95% pure. This sample was not subjected to Q-sepharose anion exchange chromatography due to a suitable high level of purity.

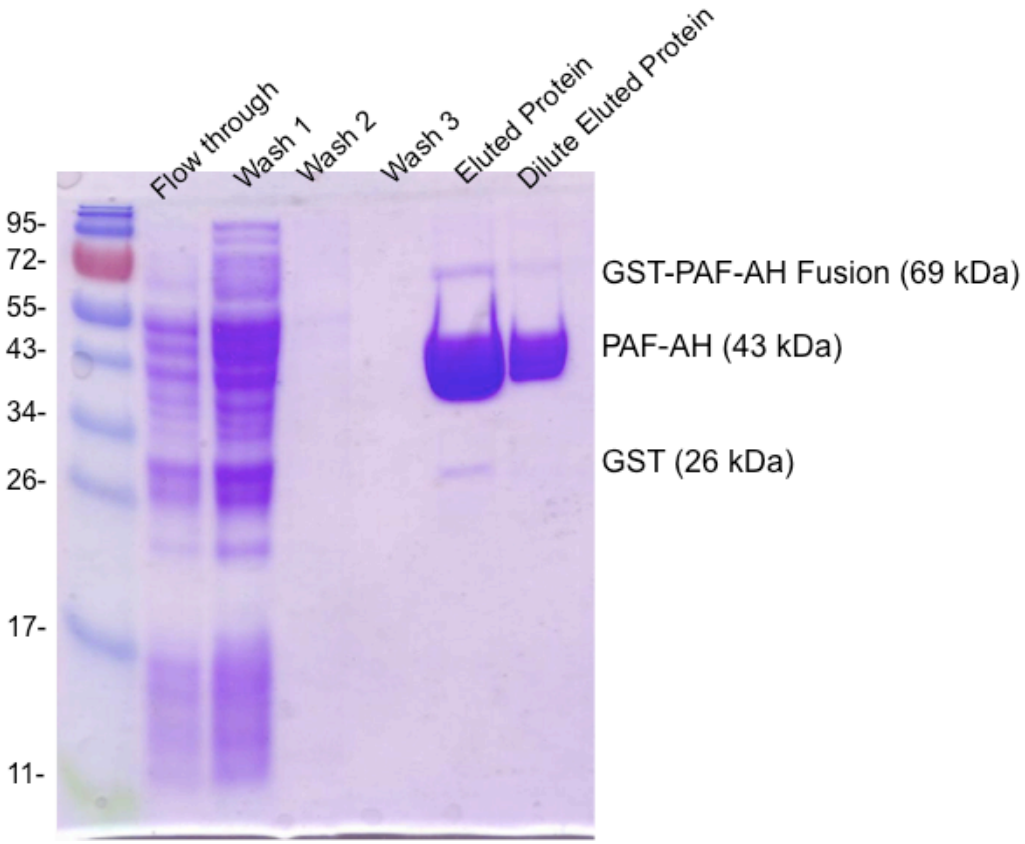

Figure 3.8 SDS Page analysis of PAF-AH after purification using a glutathione sepharose column, yielding 0.99mg of pure protein per liter of cell culture at approximately 95% purity.

The results obtained from the expression and purification of these mutant constructs of PAF-AH indicate that the cis peptide bond located between Phe-72 and Asp-73 may play a role in protein folding and overall

protein yield. The expression of mutants D73G and F72G/D73G produced a significantly more visible band at the expected molecular weight of GST-PAF-AH fusion protein when compared to wild type PAF-AH (Figure 3.2). Also, these constructs yielded a greater than 2-fold amount of pure protein product when compared to PAF-AH (Table 3.2). This enhanced expression and increased protein yield could be explained by the presence of a trans-peptide bond at this site in the mutant constructs. A trans peptide bond between residues 72 and 73 could simplify the folding kinetics of the expressed protein and eliminate a transient population of partially folded intermediates. Ideally, this would create a more homogenous protein sample that is capable of producing diffraction quality crystals. However, taking into consideration the work of Pappenberger[1], Dodge[2], and Wu[3] and their studies of tendamistat, ribonuclease A, and tryptophan synthase, it is also possible that the cis conformation is conserved in the mutated constructs. In all three cases, a cis prolyl residue was mutated to either glycine or alanine and the presence of a cis peptide bond at that site was conserved. It is also worth noting that in all three cases the conserved cis peptide bond was located in a β turn. It is proposed that tight overlapping β turns in which the peptide chain folds back on itself are stabilizing to the formation of a cis peptide bond. Taking into consideration that the cis peptide bond of PAF-AH is also located in a

β turn, it is likely that the presence of a cis peptide bond at this site is conserved despite mutagenesis. If the cis-peptide bond remains in the D73G and F72G/D73G constructs, then the enhanced protein expression and increased protein yield could be explained by mutation due to the fact that glycine residues are simply smaller than phenylalanine and aspartate and are able to isomerize into the cis conformation more easily with decreased steric hindrance between the side chains. The expression of the double mutant construct F72E/D73G produced similar quantities of fusion protein (Figure 3.2) and very similar quantities of pure protein product (Table 3.2) when compared to wild type PAF-AH. Since the construct F72E/D73G expresses very similarly to PAF-AH, it can be inferred that there were no major changes to protein structure and that residues 72 and 73 likely remain in the cis conformation despite mutagenesis.

Table 3.2 Pure protein yields of PAF-AH and mutated PAF-AH constructs

PAF-AH Construct	Protein Yield (mg/ L)
PAF-AH	0.99
D73G	2.47*
F72G/D73G	2.49
F72E/D73G	1.07

*Protein yield before purification with Q-Sepharose anion exchange was included for D73G due to high degree of protein loss.

The specific activity of PAF-AH, D73G, F72G/D73G, and F72E/D73G was determined through the use of PNPA as a substrate as described in section 3.7. The experimentally determined specific activity values of PAF-AH and PAF-AH mutant constructs were all found to have relatively similar values (Figure 3.9). This indicates that mutagenesis at residues 72 and 73 did not distort the active site of the protein and that fully folded protein samples were still attainable after mutagenesis.

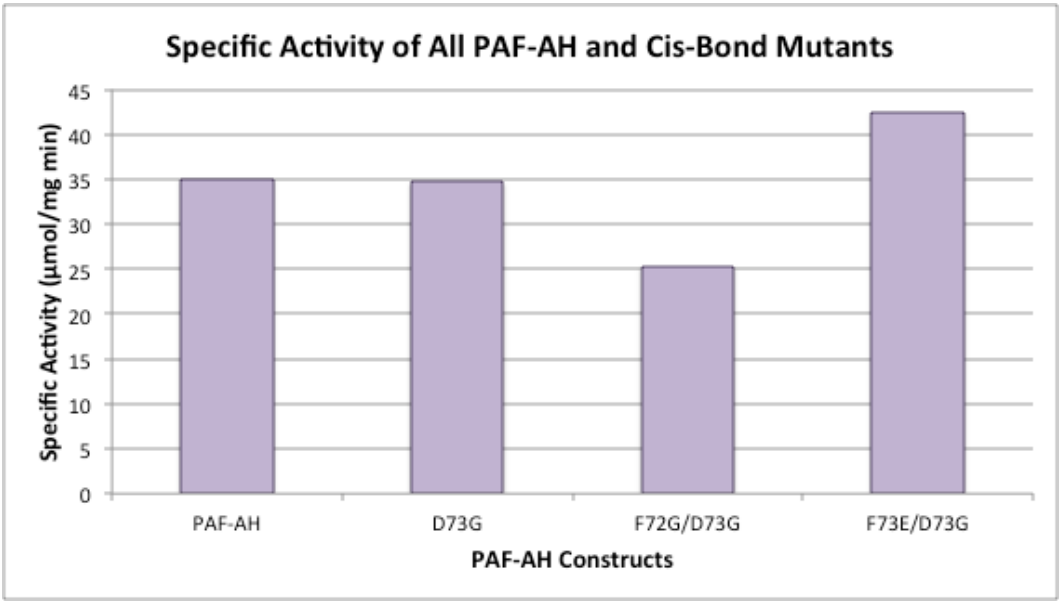

Figure 3.9 Specific activity of PAF-AH and mutated PAF-AH constructs determined using PNPA as a substrate. The experimentally determined specific activity values are as follows: PAF-AH= 35.04 μ mol/mgmin, D73G= 34.68 μ mol/mgmin, F72G/D73G= 25.26 μ mol/mgmin, and F72G/D73G= 42.45 μ mol/mgmin.

REFERENCES

1. Pappenberger, G., Aygun, H., Engels, J., Reimer, U., Fischer, G., Kiefhaber, T. (2001) Nonprolyl cis peptide bonds in unfolded proteins cause complex folding kinetics. *Nat. Struct. Biol. 8,* 452-458.

2. Dodge, R. W., Scheraga, H. A. (1996) Folding and unfolding kinetics of the proline-to-alanine mutants of bovine pancreatic ribonuclease A. *Biochemistry*. *35,* 1548-1559.

3. Wu, Y., Matthews, R. (2002) A cis-prolyl peptide bond isomerization dominates the folding of the alpha subunit of Trp synthase, a TIM barrel protein. *J. Mol. Biol*. *322,* 7-13.

Chapter 4

EXPRESSION AND PURIFICATION OF PAF-AH MUTANTS FOR POTENTIAL SOMANASE ACTIVITY

4.1 Introduction

Soman (GD) is a nerve agent that interferes with a normally functioning mammalian nervous system by inhibiting acetylcholinesterase and butyrylcholinesterase. Soman is part of the G-series of nerve agents that were produced by German scientists during World War II, which also include tabun (GA), sarin (GB), and cyclosarin (GF). The production of soman is rigorously controlled due to its classification as a weapon of mass destruction by the United Nations according to UN Resolution 687[1].

Soman as well as other organophosphorous (OP) compounds has been shown to inactivate a larger superfamily of serine hydrolases, including PAF-AH. This can occur when the nucleophillic serine residue reacts with OPs through an S_N2 mechanism with a trigonal bipyramidal

transition state. Once the leaving group is displaced, the chiral phosphorous atom undergoes stereoinversion. This complex can yield several different results depending on the enzyme in question, which include: maintenance of the stable complex, reactivation through either hydrolysis or a strong nucleophile, or dealkylation of the OP adduct[2, 3]. When bound to acetylcholinesterase OP compounds with branched side chains undergo an irreversible dealkylation process known as aging. Following the aging process, acetylcholinesterase cannot be reactivated by nucleophiles to regenerate enzymatic activity[4,5]. Therefore, recent efforts have focused on engineering serine hydrolase enzymes to hydrolyze OP nerve agents and function as catalytic OP bioscavengers[6]. Plasma PAF-AH is an interesting target to examine for OP hydrolysis reactivity due to its presence in human blood. This is an ideal site for the detoxification of OPs because nerve agents reach nerve synapse acetylcholinesterase via the bloodstream.

The crystal structure of PAF-AH following inhibition with soman has been solved and modeled with two stereoisomers of soman, P_RC_S and P_SC_S (Figure 4.1). The presence of P_R and P_S stereoisomers shows that the soman complex does not age unlike acetylcholinesterase complexes with sarin, soman, and disopropylfluorophosphate (DFP)[2]. This discrepancy is likely due to the absence of a mobile catalytic histidine to

carry out the proton transfer and a solvent accessible active site in PAF-AH. For example, in the case of PAF-AH His-351 is restricted in movement by surrounding residues and by the alkyl group of the bound soman. Also unlike acetylcholinesterase, the hydrophobic alkyl group of the bound soman blocks water molecules from interacting with the active site of PAF-AH.

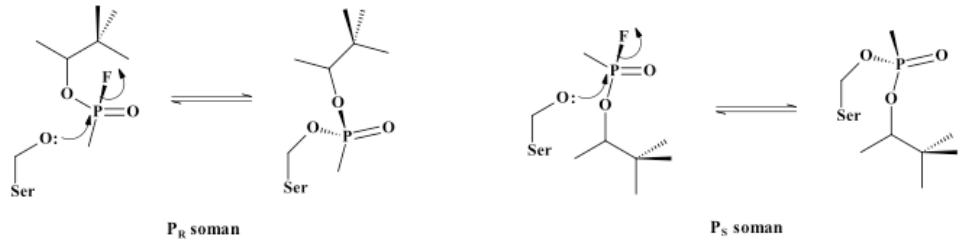

Figure 4.1 The reaction of P_RC_S and P_SC_S isomers of soman with Ser-273 of PAF-AH to show the formation of a non-aged complex.

Currently, there are two predominant methods through which treatments against OP poisoning are successful. Through the first method, a compound is administered that could be rapidly phosphorylated and effectively protects acetylcholinesterase from inhibition by competing with it for OP binding. Through the second method, a compound is administered that could restore the activity of inhibited acetylcholinesterase through dephosphorylation[8]. However, clinical experiences with these treatments have been disappointing. While the

current treatments against OP poisoning are effective, they can produce severe side effects as well as behavioral incapacitation if they are given in large doses or if they are administered beyond the prescribed time frame after OP exposure[9]. These unwanted side effects have motivated recent efforts in which enzymes, such as PAF-AH, are engineered to hydrolyze nerve agents before they reach their acetylcholinesterase targets. For the purpose of generating novel OP hydrolase activity, a histidine mutation was created near the permissive active site of plasma PAF-AH. This mutation, W2989H, was found to display novel somanase activity with a k_{cat} of 5 min^{-1} and a K_M of 590 μ M at pH 7.5. The success of this mutation is believed to be due the ideal location of residue 298 within the active site. This mutation allows histidine to act as a general base catalyst and activate a water molecule for addition onto the appropriate face of the phosphor-enzyme intermediate[10].

In an attempt to further enhance the somanase activity of plasma PAF-AH, two additional mutations were created, W298H/F300D and W298H/F300E (Figure 4.2). These mutations may facilitate the formation of a catalytic triad in which a nucleophillic serine residue (Ser-273) is activated by a proton relay involving an acidic residue (Asp-300/Glu-300) and a basic residue (His-298). Ideally with this catalytic triad in place, the hydrolysis of soman by plasma PAF-AH will be further enhanced.

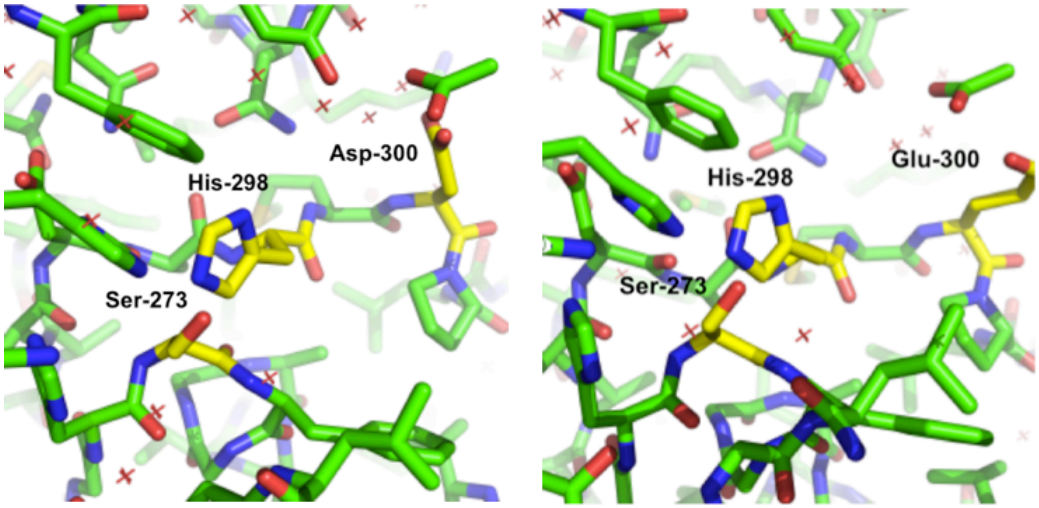

Figure 4.2 Stick diagram of D73G/W298H/F300D and D73G/W298H/F300E mutations featuring Ser-273, His-298, and Asp/Glu-300 highlighted in yellow.

The isoelectric point of each PAF-AH construct was calculated using ExPASy Compute pI tool. The predicted isoelectric point of PAF-AH and mutant construct D73G/W298H was calculated to be 6.97 (Table 4.1). Therefore, to ensure a net negative charge of the protein and solubility, a pH 8.1 buffering system was used for all purification steps. The predicted isoelectric point for mutant constructs D73G/W298H/F300D and D73G/W298H/F300E was calculated to be 6.72 and a pH 7.8 buffering system was used for all purification steps.

Table 4.1 Predicted pI of mutated PAF-AH constructs

PAF-AH Construct	Predicted pI
D73G	6.95
D73G/W298H	6.97
D73G/W298H/F300D	6.72
D73G/W298H/F300E	6.72

4.2 Production of D73G/W298H, D73G/W298H/F300D, and D73G/W298H/F300E

D73G in pGEX-6P1 was used as a plasmid DNA template to mutate the 298th residue of PAF-AH from tryptophan to histidine and 300th residue from phenylalanine to either aspartate or glutamate through site directed mutagenesis. The PCR procedure was performed using 1 μL plasmid DNA (30 ng/μL), 1.5 μL forward primer, 1.5 μL reverse primer, 2 μL dNTP mix, 5 μL 10x reaction buffer, and 1 μL pfu Ultra DNA polymerase. Site directed mutagenesis was performed using the following primers:

D73G/W298H

Forward: 5’ GCCCTGGATGCACATATGTTTCCACTGGG 3’

Reverse: 5’ CCCAGTGGAAACATATGTGCATCCAGGGC 3’

D73G/W298H/F300D

Forward: 5’ GATGCACATATGGATCCACTGGGTGATG 3’

Reverse: 5’ CATCACCCAGTGGATCCATATGTGCATC 3’

D73G/W298H/F300E

Forward: 5’ GATGCACATATGGAACCACTGGGTGATG 3’

Reverse: 5’ CATCACCCAGTGGTTCCATATGTGCATC 3’

Gradient PCR was performed to determine the optimal annealing temperature for this set of mutagenic primers. The annealing temperatures of this gradient were selected to be lower than the Tm of the primer set (78.8 °C, 74.8 °C, and 74.7 °C respectively) and comprised of annealing temperatures ranging from 60-70 °C. The optimal annealing temperature was shown to be 65 °C and mutant constructs D73G/W289H, D73G/W298H/F300D, and D73G/W298H/F300E were produced using the following PCR parameters (Figure 4.3):

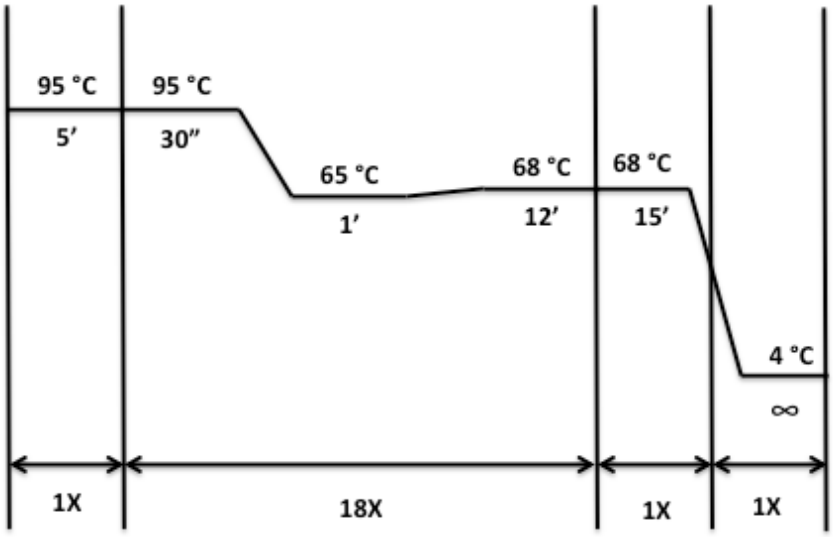

Figure 4.3 Optimal PCR cycle parameters to produce mutant constructs D73G/W298H, D73G/W298H/F300D, and D73G/W298H/F300E.

The mutagenic products were digested with DPN1 and transformed into DH5α and BL21 chemically competent cells. Clones were grown in 5 mL of culture, purified using QIAprep Spin Miniprep Kit (Qiagen), and sent out for DNA sequencing (Genewiz; South Plainfield, NJ). The production of mutant constructs D73G/W298H, D73G/W298H/F300D, and D73G/W298H/F300E were confirmed through DNA sequencing. These sequencing results were then used to perform a sequence alignment between the mutant constructs and D73G (Figure 4.4) using Culstal Omega software.

Figure 4.4 DNA sequence alignment between D73G/W298H, D73G/W298H/F300D, D73G/W298H/F300E and D73G showing mutation at Trp-298 and Phe-300. Affected residues are boxed to show mutation.

4.3 Expression and Purification of D73G/W298H, D73G/W298H/F300D, and D73G/W298H/F300E

D73G/W298H, D73G/W298H/F300D, and D73G/W298H/F300E were expressed in *E. coli* (strain BL21) and induced with 1 mM IPTG after 5 h of growth. SDS-PAGE analysis was performed on whole cells obtained before and after induction with IPTG. The cells were lysed with SDS-PAGE sample buffer to visualize the relative quantities of expressed fusion protein (Figure 4.5). Through this analysis, it was shown that mutant constructs D73G/W298H and D73G/W298H/F300E produce greater quantities of fusion protein when compared to D73G/W298H/F300D. This

could be seen through the presence of a much darker band in lanes corresponding to induced D73G/W298H and D73G/W298H/F300E at the expected molecular weight of fusion protein (69 kDa) when compared to D73G/W298H/F300D.

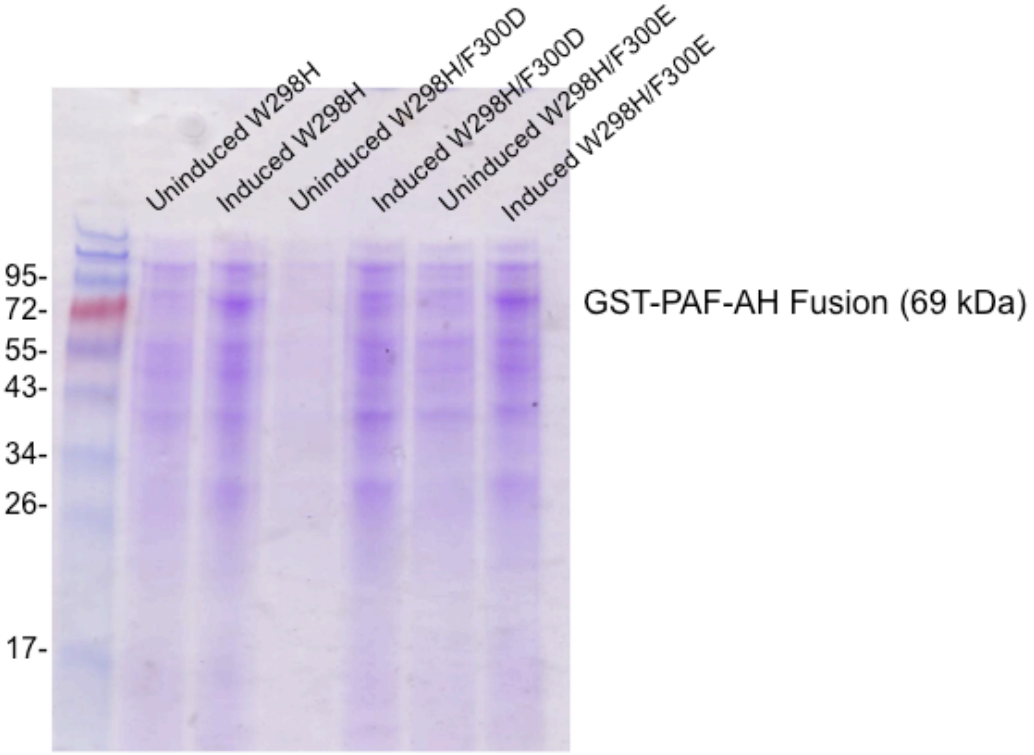

Figure 4.5 SDS PAGE analysis of whole cell expression of D73G/W298H, D73G/W298H/F300D, and D73G/W298H/F300E before and after induction with 1 mM IPTG. Molecular weight of fusion protein =69 kDa.

Mutant construct D73G/W298H was purified using a pH 8.1 buffering system in accordance with its predicted pI of 6.97. W298H was purified using a glutathione Sepharose column, yielding 1.21 mg of

recombinant protein per liter of cell culture (Figure 4.6). The purity of the resulting protein SDS PAGE sample was quantitated using ImageJ software and was found to be approximately 73% pure.

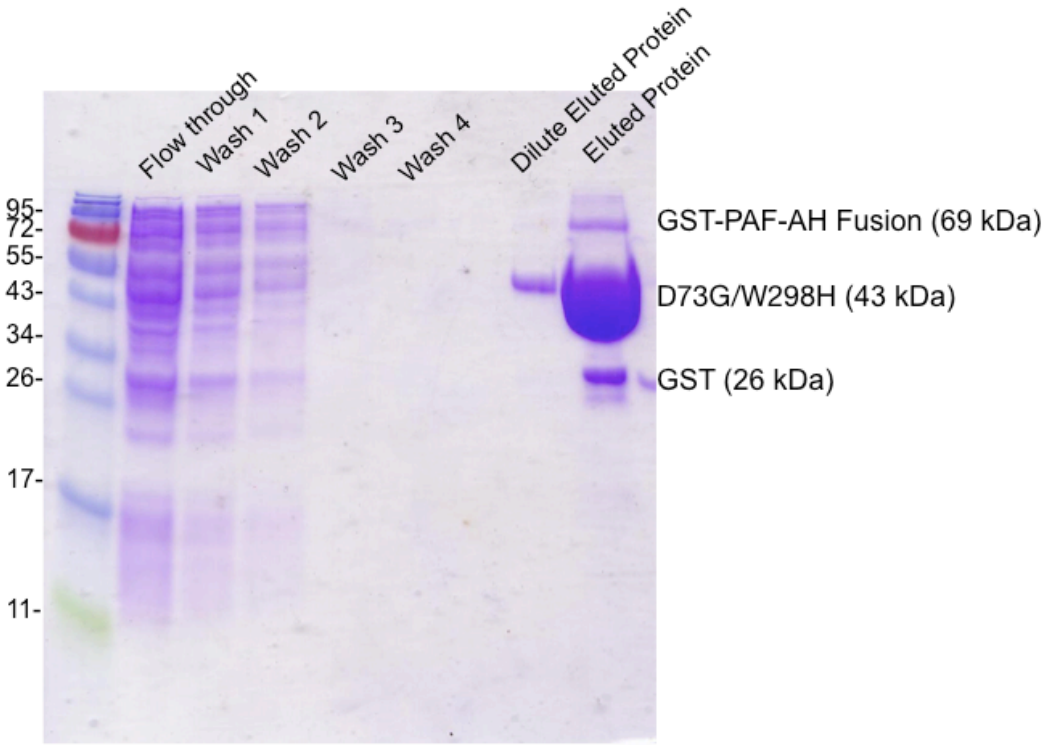

Figure 4.6 SDS Page analysis of D73G/W298H after purification using a Glutathione Sepharose column, yielding 1.21 mg of protein per liter of cell culture at approximately 73% purity.

Mutant constructs D73G/W298H/F300D and D73G/W298H/F300E were purified using a pH 7.8 buffering system in accordance with its predicted pI of 6.72. D73G/W298H/F300D was purified using a Glutathione Sepharose column, yielding 0.053 mg of recombinant protein per liter of cell culture (Figure 4.7). The purity of the resulting protein SDS

PAGE sample was quantitated using ImageJ software and was found to be approximately 19% pure.

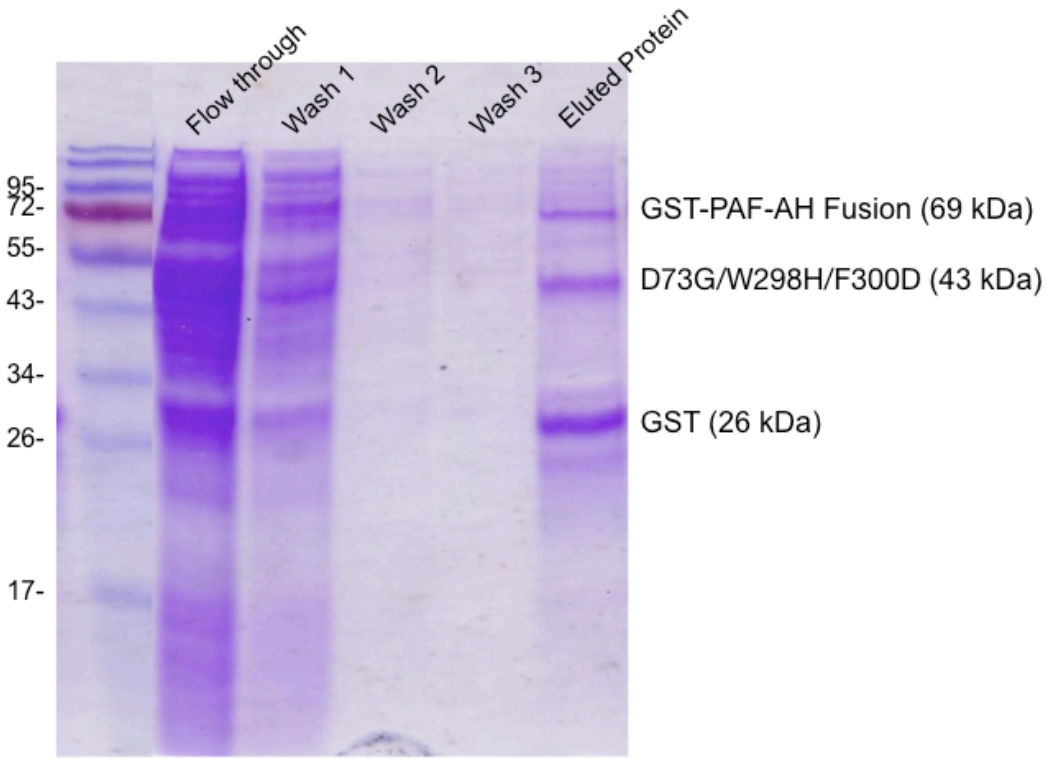

Figure 4.7 SDS Page analysis of D73G/W298H/F300D after purification using a Glutathione Sepharose column, yielding 0.053 mg of protein per liter of cell culture at approximately 19% purity.

D73G/W298H/F300E was purified using a Glutathione Sepharose column, yielding 0.72 mg of recombinant protein per liter of cell culture (Figure 4.8). The purity of the resulting protein SDS PAGE sample was quantitated using ImageJ software and was found to be approximately 67% pure.

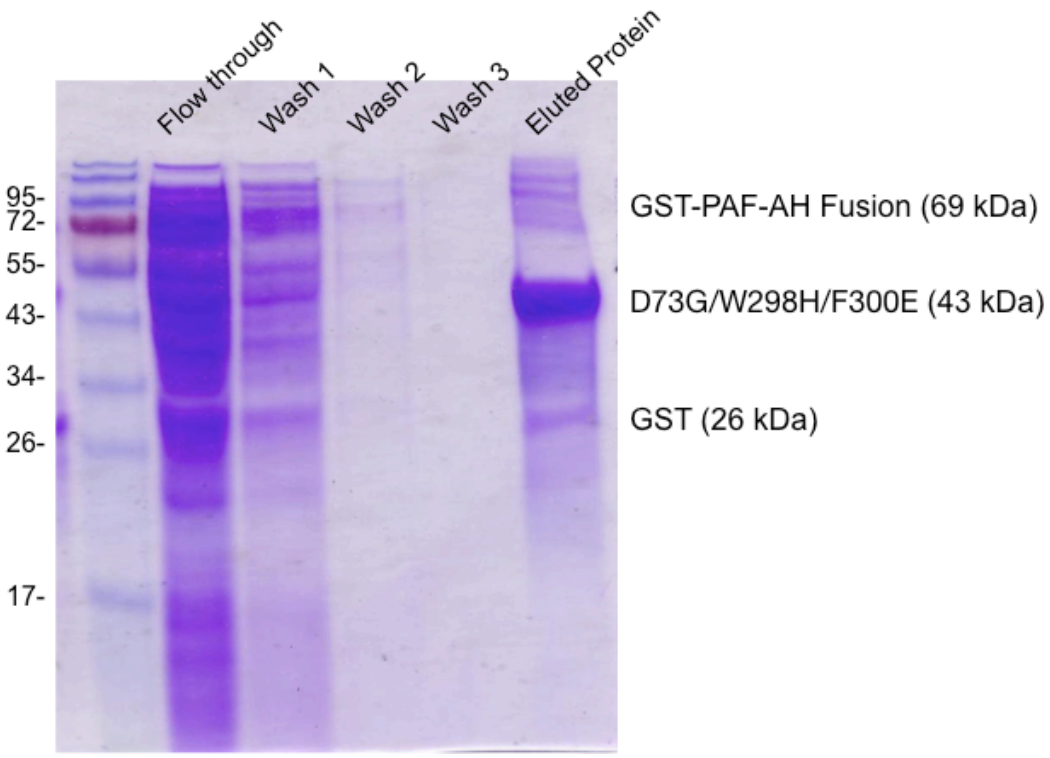

Figure 4.8 SDS Page analysis of D73G/W298H/F300E after purification using a Glutathione Sepharose column, yielding 0.72 mg of protein per liter of cell culture at approximately 67% purity.

The results obtained from the expression and purification of these mutant constructs of PAF-AH indicated that mutagenesis of Trp-298 and Phe-300 dramatically decrease protein expression and pure protein yield. For example, the expression and purification of mutant constructs D73G/W298H and D73G/W298H/F300E yielded less than half of the amount of pure protein product when compared to D73G (Table 4.2). Furthermore, the expression and purification of D73G/W298H/F300D had a very low yield. Additionally, whole cell SDS-PAGE analysis after

induction with IPTG revealed that the expression of mutants D73G/W298H and D73G/W298H/F300E produced a significantly more visible band at the expected molecular weight of fusion protein when compared to D73G/W298H/F300D (Figure 4.5). These results suggest that while protein expression and overall folding can tolerate some degree of mutagenesis at Trp-298 and Phe-300, the substitution of Phe-300 for aspartate appears to destabilize the folded protein and impede protein expression.

Table 4.2 Pure protein yields of PAF-AH and mutated Δ PAF-AH constructs

PAF-AH Construct	Protein Yield (mg/ L)
D73G	2.47*
D73G/W298H	1.21
D73G/W298H/F300D	0.053
D73G/W298H/F300E	0.72

*Protein yield before purification with Q-Sepharose anion exchange was included for D73G due to high degree of protein loss.

The specific activity of D73G/W298H, D73G/W298H/F300D, D73G/W298H/F300E was determined through the use of PNPA as a substrate as described in section 3.7. The experimentally determined specific activity values of D73G/W298H, D73G/W298H/F300D, D73G/W298H/F300E were all found to be significantly lower than D73G (Figure 4.9). This indicates that mutagenesis at residues 298 and 300 may distort the active site of the protein. In particular, the experimentally determined specific activity of D73G/W298H/F300D is reasonably low when compared to D73G/W298H and D73G/W298H/F300D, suggesting that the mutagenesis of Phe-300 for aspartate is not tolerated and may be destabilizing to the folded protein. However, mutant construct D73G/W298H/F300E is of particular interest. Due to its similar expression, pure protein yield, and specific activity when compared to D73G/W298H, this construct is an acceptable choice for additional testing for Somanase activity.

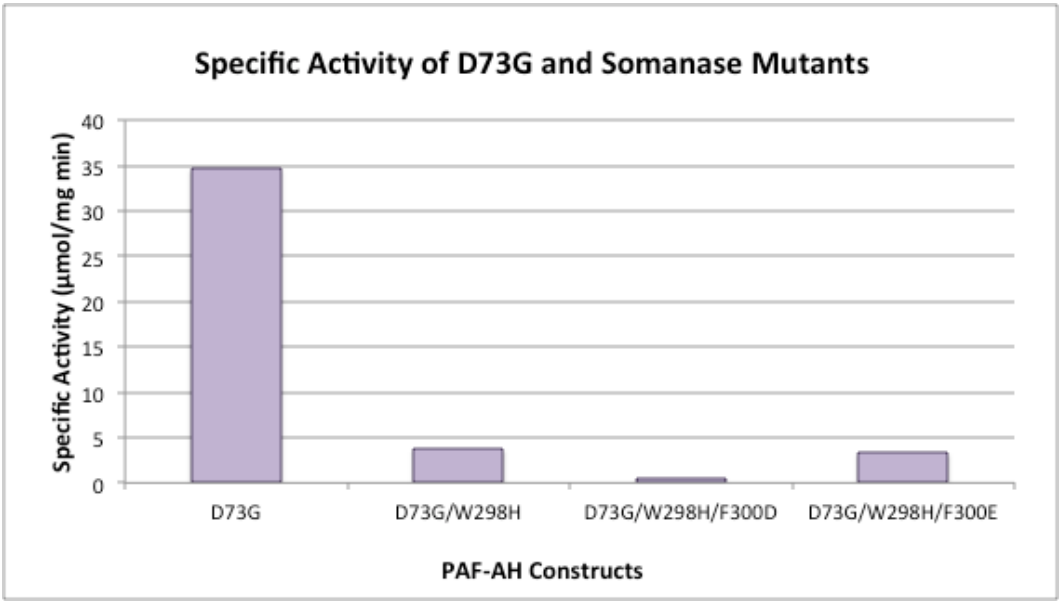

Figure 4.9 Specific activity of D73G and mutated PAF-AH constructs determined using PNPA as a substrate. The experimentally determined specific activity values are as follows: D73G= 34.68 μ mol/mgmin, D73G/W298H= 3.70 μ mol/mgmin, D73G/W298H/F300D= 0.47 μ mol/mgmin, and D73G/W298H/F300E= 3.26 μ mol/mgmin.

REFERENCES

1. Holstege, C. P., Kirk, M., Sidell, F. R. (1997) Chemical warfare. Nerve agent poisoning. *Crit Care Clin*. *13,* 923-942.

2. Millard, C. B., Kryger, G., Ordentlich, A. (1999) Crystal structures of aged phosphonylated acetylcholinesterase: nerve agent reaction products at the atomic level. *Biochemistry*. *38,* 7032-7039.

3. Casida, J. E., Quistad, G. B. (2004) Organophosphate toxicology: safety aspects of nonacetylcholinesterase secondary targets. *Chem. Res. Toxicol*. *17,* 983-998.

4. Michel, H. O., Hackley, B. E., Berkowitz, I., List, G., Hackley, E. B., Gilliam, W. (1967) Ageing and dealkylation of Soman (pinacolylmethylphosphonofluoridate)-inactivated eel cholinesterase. *Arch. Biochem. Biophy*s. *121,* 29-34.

5. Harris, L. W., Fleisher, J. H., Clark, J., Cliff, W. F., (1966) Dealkylation and loss of capacity for reactivation of cholinesterase inhibited by sarin. *Science*. *154,* 404-407.

6. Broomfield, C. A., Lockridge, O., Millard, C.B. (1999) Protein engineering of a human enzyme that hydrolyzes V and G nerve agents: design, construction and characterization. *Chem. Biol. Interact*. *119-120,* 413-418.

7. Samanta, U., Kirby, S., Srinivasan, P., Cerasoli, D. M., Bahnson, B. J. (2009) Crystal structures of human group-VIIA phospholipase A2 inhibited by organophosphorus nerve agents exhibit non-aged complexes. *Biochemical Pharmacology*. *78,* 420-429.

8. Davies, D. R., Green, A. L. (1958) The chemotherapy of poisoning by organophosphate anticholinesterases. *Brit. J. Industr. Med*. *16,* 128-134.

9. Lorke, D. E., Hasan, M. Y., Arafat, K., Kuca, K., Musilek, K., Schmitt, A., Petroianu, G. A. (2008) In vitro oxime protection of human red blood cell acetylcholinesterase inhibited by diisopropyl-fluorophosphate. *J. Appl. Toxicol*. *28,* 422-429.

10. Kirby, S. D., Norris, J., Sweeney, R., Bahnson, B. J., Cerasoli, D. M. (2015). A Rationally Designed Mutant of Plasma Platelet-Activating Factor Acetylhydrolase Hydrolyzes Organophosphorous Nerve Agents. Unpublished.

Appendix

REPRINT PERMISSION

SPRINGER LICENSE
TERMS AND CONDITIONS

Apr 26, 2015

This is a License Agreement between Kaitlyn M Woerner ("You") and Springer ("Springer") provided by Copyright Clearance Center ("CCC"). The license consists of your order details, the terms and conditions provided by Springer, and the payment terms and conditions.

All payments must be made in full to CCC. For payment instructions, please see information listed at the bottom of this form.

License Number	3577710851875
License date	Feb 28, 2015
Licensed content publisher	Springer
Licensed content publication	Amino Acids
Licensed content title	Cis–trans peptide variations in structurally similar proteins
Licensed content author	Agnel Praveen Joseph
Licensed content date	Jan 1, 2012
Volume number	43
Issue number	3
Type of Use	Thesis/Dissertation
Portion	Figures
Author of this Springer article	No
Order reference number	None
Original figure numbers	Figures 1, 3
Title of your thesis / dissertation	EXPRESSION AND PURIFICATION OF NON-PROLYL CIS-PEPTIDE BOND MUTANTS IN HUMAN PLASMA PLATELET ACTIVATING FACTOR ACETYLHYDROLASE
Expected completion date	Jun 2015
Estimated size(pages)	75
Total	0.00 USD
Terms and Conditions	

Introduction

The publisher for this copyrighted material is Springer Science + Business Media. By clicking "accept" in connection with completing this licensing transaction, you agree that the following terms and conditions apply to this transaction (along with the Billing and Payment terms and conditions established by Copyright Clearance Center, Inc. ("CCC"), at the time that you opened your Rightslink account and that are available at any time at http://myaccount.copyright.com).

Limited License

With reference to your request to reprint in your thesis material on which Springer Science

and Business Media control the copyright, permission is granted, free of charge, for the use indicated in your enquiry.

Licenses are for one-time use only with a maximum distribution equal to the number that you identified in the licensing process.

This License includes use in an electronic form, provided its password protected or on the university's intranet or repository, including UMI (according to the definition at the Sherpa website: http://www.sherpa.ac.uk/romeo/). For any other electronic use, please contact Springer at (permissions.dordrecht@springer.com or permissions.heidelberg@springer.com).

The material can only be used for the purpose of defending your thesis limited to university-use only. If the thesis is going to be published, permission needs to be re-obtained (selecting "book/textbook" as the type of use).

Although Springer holds copyright to the material and is entitled to negotiate on rights, this license is only valid, subject to a courtesy information to the author (address is given with the article/chapter) and provided it concerns original material which does not carry references to other sources (if material in question appears with credit to another source, authorization from that source is required as well).

Permission free of charge on this occasion does not prejudice any rights we might have to charge for reproduction of our copyrighted material in the future.

Altering/Modifying Material: Not Permitted
You may not alter or modify the material in any manner. Abbreviations, additions, deletions and/or any other alterations shall be made only with prior written authorization of the author(s) and/or Springer Science + Business Media. (Please contact Springer at (permissions.dordrecht@springer.com or permissions.heidelberg@springer.com)

Reservation of Rights
Springer Science + Business Media reserves all rights not specifically granted in the combination of (i) the license details provided by you and accepted in the course of this licensing transaction, (ii) these terms and conditions and (iii) CCC's Billing and Payment terms and conditions.

Copyright Notice:Disclaimer
You must include the following copyright and permission notice in connection with any reproduction of the licensed material: "Springer and the original publisher /journal title, volume, year of publication, page, chapter/article title, name(s) of author(s), figure number(s), original copyright notice) is given to the publication in which the material was originally published, by adding; with kind permission from Springer Science and Business Media"

Warranties: None

Example 1: Springer Science + Business Media makes no representations or warranties with respect to the licensed material.

Example 2: Springer Science + Business Media makes no representations or warranties with respect to the licensed material and adopts on its own behalf the limitations and disclaimers

established by CCC on its behalf in its Billing and Payment terms and conditions for this licensing transaction.

Indemnity
You hereby indemnify and agree to hold harmless Springer Science + Business Media and CCC, and their respective officers, directors, employees and agents, from and against any and all claims arising out of your use of the licensed material other than as specifically authorized pursuant to this license.

No Transfer of License
This license is personal to you and may not be sublicensed, assigned, or transferred by you to any other person without Springer Science + Business Media's written permission.

No Amendment Except in Writing
This license may not be amended except in a writing signed by both parties (or, in the case of Springer Science + Business Media, by CCC on Springer Science + Business Media's behalf).

Objection to Contrary Terms
Springer Science + Business Media hereby objects to any terms contained in any purchase order, acknowledgment, check endorsement or other writing prepared by you, which terms are inconsistent with these terms and conditions or CCC's Billing and Payment terms and conditions. These terms and conditions, together with CCC's Billing and Payment terms and conditions (which are incorporated herein), comprise the entire agreement between you and Springer Science + Business Media (and CCC) concerning this licensing transaction. In the event of any conflict between your obligations established by these terms and conditions and those established by CCC's Billing and Payment terms and conditions, these terms and conditions shall control.

Jurisdiction
All disputes that may arise in connection with this present License, or the breach thereof, shall be settled exclusively by arbitration, to be held in The Netherlands, in accordance with Dutch law, and to be conducted under the Rules of the 'Netherlands Arbitrage Instituut' (Netherlands Institute of Arbitration).***OR:***

All disputes that may arise in connection with this present License, or the breach thereof, shall be settled exclusively by arbitration, to be held in the Federal Republic of Germany, in accordance with German law.

Other terms and conditions:

v1.3

Questions? customercare@copyright.com or +1-855-239-3415 (toll free in the US) or +1-978-646-2777.

Gratis licenses (referencing $0 in the Total field) are free. Please retain this printable license for your reference. No payment is required.